(12) INTERNATIONAL APPLICATION PUBLISHED UNDER THE PATENT COOPERATION TREATY (PCT)

(19) World Intellectual Property Organization
International Bureau

(43) International Publication Date
14 February 2008 (14.02.2008)

PCT

(10) International Publication Number
WO 2008/019291 A2

(51) International Patent Classification:
A61K 39/395 (2006.01)

(21) International Application Number:
PCT/US2007/075083

(22) International Filing Date: 2 August 2007 (02.08.2007)

(25) Filing Language: English

(26) Publication Language: English

(30) Priority Data:
60/821,454 4 August 2006 (04.08.2006) US

(71) Applicant *(for all designated States except US)*: **BOARD OF REGENTS, THE UNIVERSITY OF TEXAS SYSTEM** [US/US]; 201 West 7th Street, Austin, TX 78701 (US).

(72) Inventors; and
(75) Inventors/Applicants *(for US only)*: **KUANG, Jian** [CN/US]; 3617 Timberside Circle Dr., Houston, TX 77025 (US). **ZHOU, Xi** [CN/US]; 7900 Cambridge Street #28-2F, Houston, TX 77054 (US). **PAN, Shujuan** [CN/US]; 13231 Thornoak Lane, Houston, TX 77070 (US). **WANG, Ruoning** [CN/US]; 7900 Cambridge Street #15-2C, Houston, TX 77054 (US).

(74) Agent: **MORICO, Paul, R.**; Baker Botts L.L.P., 910 Louisiana Street, Houston, TX 77002-4995 (US).

(81) Designated States *(unless otherwise indicated, for every kind of national protection available)*: AE, AG, AL, AM, AT, AU, AZ, BA, BB, BG, BH, BR, BW, BY, BZ, CA, CH, CN, CO, CR, CU, CZ, DE, DK, DM, DO, DZ, EC, EE, EG, ES, FI, GB, GD, GE, GH, GM, GT, HN, HR, HU, ID, IL, IN, IS, JP, KE, KG, KM, KN, KP, KR, KZ, LA, LC, LK, LR, LS, LT, LU, LY, MA, MD, ME, MG, MK, MN, MW, MX, MY, MZ, NA, NG, NI, NO, NZ, OM, PG, PH, PL, PT, RO, RS, RU, SC, SD, SE, SG, SK, SL, SM, SV, SY, TJ, TM, TN, TR, TT, TZ, UA, UG, US, UZ, VC, VN, ZA, ZM, ZW.

(84) Designated States *(unless otherwise indicated, for every kind of regional protection available)*: ARIPO (BW, GH, GM, KE, LS, MW, MZ, NA, SD, SL, SZ, TZ, UG, ZM, ZW), Eurasian (AM, AZ, BY, KG, KZ, MD, RU, TJ, TM), European (AT, BE, BG, CH, CY, CZ, DE, DK, EE, ES, FI, FR, GB, GR, HU, IE, IS, IT, LT, LU, LV, MC, MT, NL, PL, PT, RO, SE, SI, SK, TR), OAPI (BF, BJ, CF, CG, CI, CM, GA, GN, GQ, GW, ML, MR, NE, SN, TD, TG).

Published:
— *without international search report and to be republished upon receipt of that report*

(54) Title: ANTI-ALIX ANTIBODIES AND HYBRIDOMAS

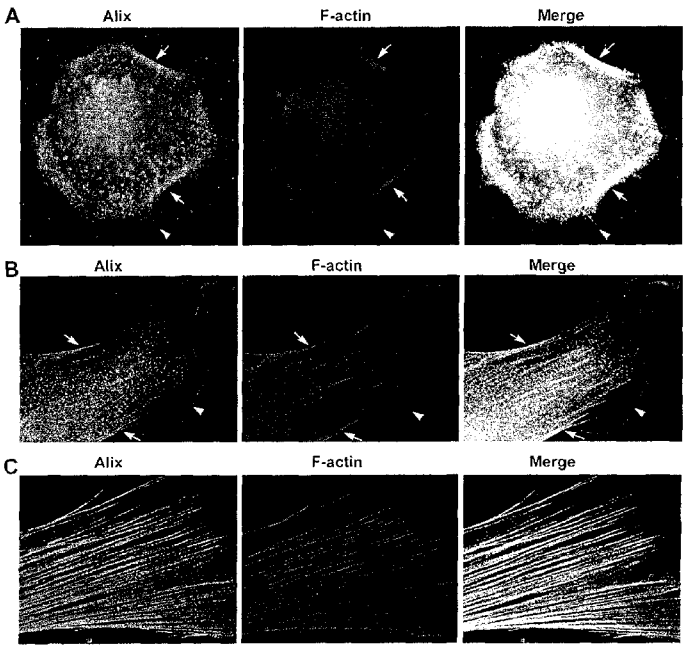

(57) Abstract: The present disclosure, according to specific example embodiments, generally relates to production and methods of use of antibodies. In particular, the present disclosure relates to anti-Alix antibodies and associated methods of using such antibodies in studies relating to Alix, including but not limited to properties such as the structure, function, and distribution of Alix in cells or in a suspension.

WO 2008/019291 A2

ANTI-ALIX ANTIBODIES AND HYBRIDOMAS

CROSS-REFERENCE TO RELATED APPLICATION

This application claims the benefit of U.S. Provisional Application Serial No. 60/821,454 filed on August 4, 2006, which is incorporated by reference.

STATEMENT OF GOVERNMENT INTEREST

This invention was made with government support under Grant No. CA093941 awarded by the National Institute of Health. The U.S. Government has certain rights in the invention.

BACKGROUND

Alix/AIP1 (ALG-2 interacting protein X or 1) is the mammalian ortholog of an evolutionally conserved family of adaptor proteins. These proteins are characterized by an N-terminal Bro1 domain and a C-terminal proline-rich domain (PRD), both of which mediate protein-protein interactions (8). Previous studies have demonstrated that Alix interacts with a variety of cytoplasmic proteins in addition to the EF-hand calcium binding protein ALG-2, including the ubiquitin ligase-like protein TSG-101 (76), the endosomal membrane-associated protein CHMP4b (51, 52), the lysophosphatidic acid acyltransferase endophillin (41), the SH3-domian containing protein CIN85/SETA (42). Alix interactions with these partner proteins regulate apoptotic signaling (58, 74), endocytosis (69) or multivesicular body (MVB) sorting of endocytosed transmembrane proteins (53, 61, 76). In order to study and understand the structure and function of Alix in the intracellular and extracellular environment, anti-Alix antibodies have been developed.

SUMMARY

The present disclosure, according to specific example embodiments, generally relates to production and methods of use of antibodies. In particular, the present disclosure relates to anti-Alix antibodies and associated methods of using such antibodies in studies relating to Alix, including but not limited to properties such as the structure, function, and distribution of Alix in cells or in a suspension.

DRAWINGS

Some specific example embodiments of the disclosure may be understood by referring, in part, to the following description and the accompanying drawings.

Figure 1 shows that Alix is required for WI38 cells to maintain typical fibroblast morphology. (A) Immunoblots of Alix (top panel) and actin (bottom panel) in crude lysates of control or Alix siRNA-transfected WI38 cells collected at 24, 48, 72, and 96 hrs after the transfection. (B) Phase contrast images of control or Alix siRNA-transfected WI38 cells at 48 hrs after the transfection (upper panel) or that had been subcultured at 24 hrs after the transfection and further cultured for 24 hrs (lower panel).

Figure 2 shows that Alix associates with actin cytoskeleton in WI38 cells. WI38 cells that had been cultured for 1 hr (A) or 24 hrs (B) on non-treated glass coverslips, or 24 hrs on glass coverslips pre-coated with fibronectin (C) were stained with 3A9 antibody for Alix (green) and phalloidin for F-actin (red). Arrows indicate association of Alix with stress fibers, and arrowheads indicate localization of Alix at lamellipodia or spreading lamella.

Figure 3 shows that Alix knockdown inhibits actin cytoskeleton assembly. (A) Alix siRNA-transfected cells were stained with 3A9 antibody for Alix (green) and phalloidin for F-actin (red). Arrows indicate the two cells in which Alix expression remained high, and arrowheads indicate adjacent Alix knockdown cells. (B) Phalloidin staining of F-actin in WI38 cells with or without pre-treatment with 5 μM cytochalasin D. (C) Control or Alix knockdown WI38 cells were lysed in F-actin actin stabilization buffer and fractionated by ultracentrifugation. The proteins in the G-actin containing supernatant (S) and the F-actin containing pellet (P) were immunoblotted with anti-actin antibodies (left panel), and the F-actin to G-actin ratio in control and Alix knockdown cells was determined (right panel). (D) Control and Alix siRNA transfected cells grown on fibronectin-coated substrata were double stained with phalloidin for F-actin (red) and anti-vinculin antibodies for focal adhesions (green), and fluorescence images were taken under identical conditions.

Figure 4 shows that Alix directly interacts with actin in cell free systems. (A) Coomassie blue staining of soluble (lane S) and pelletted (lane P) fractions of GST (left panel) or GST-Alix (right panel) after their incubation with actin-polymerization buffer (F-buffer) alone or the buffer

containing 10 μg actin and ultracentrifugation. The four major polypeptides of GST-Alix sample are indicated. Four major polypeptides in the GST-Alix samples are indicated. (B) Schematic illustration of the Alix portion of different GST-Alix fusion proteins, and coomassie blue staining of soluble (lane S) and pelletted (lane P) fractions of each of these proteins after incubation with actin-polymerization buffer, or the buffer containing 10 μg actin. Arrows indicate the major polypeptides in each of the GST-Alix fusion proteins. (C) Each of the indicated in vitro translates was incubated with actin-polymerization buffer (-), or the buffer containing 10 μg actin (+), and the soluble (lane S) and pelletted (lane P) fractions of the end products were immunoblotted for each of the indicated proteins. (F) Immunoblots of input actin or actin that was pulled down by immobilized GST or GST-Alix. (G) Immunoblots of actin that was pulled down by each of the indicated proteins.

Figure 5 shows that actin is a major partner protein of Alix in WI38 cells. (A) After indicated concentrations of GST-AlixΔC were incubated with actin-polymerization buffer containing 1 μM G-actin followed by ultracentrifugation, the soluble (lane S) and pelletted (lane P) fractions of the protein were separated by SDS-PAGE and stained by Coomassie blue. (B) 1 μM GST-AlixΔC was incubated with increased concentrations (0 - 8 μM) of G-actin in the actin-polymerization buffer followed by ultracentrifugation. After the proteins in the pellets and supernatants were resolved by SDS-PAGE and stained by commassie blue, the molar amounts of pelletted GST-AlixΔC against molar amounts of pelletted F-actin were quantified by densitometry and plotted with PRIZM software. (C) Serially diluted WI38 cell lysates (upper panel) and either or both of 30 μg protein lysates of WI38 cells and 200 ng GST-AlixM (bottom panel)were immunoblotted with 1F7 antibody. (D) WI38 cell lysates were incubated with actin-polymerization buffer or the buffer containing 10 μg actin, and the soluble (lane S) and pelletted (lane P) fractions of the end products were immunoblotted for Alix and stained with Ponceau S for actin. (E) Silver staining of proteins in the immunoprecipitates of crude lysates of WI38 cells with anti-Alix antibodies or mouse IgG. The bands indicated by dashes were identified by mass spectrometry.

Figure 6 shows that Alix interacts with cortactin and promotes cortactin localization to the cell periphery. (A) WI38 cells were double stained with 3A9 anti-Alix antibody (green) and

anti-cortactin antibodies (red). Arrows indicate co-localization of Alix with cortactin at lamellipodia. (B) WI38 cell lysates were immunoprecipitated with anti-Alix antibodies or mouse IgG (mIgG), and immunocomplexes were immunoblotted with anti-Alix or anti-cortactin antibodies. (C) Equal molars of the illustrated GST fusion proteins that were immobilized onto glutathione sepharose were incubated with WI38 cell lysates containing 100 μg total proteins, and bound proteins were immunoblotted with anti-cortactin antibodies. (D) Control or Alix knockdown WI38 cells that had been cultured on fibronectin-coated substrata and in serum free medium for 24 hrs were immunostained with anti-cortactin antibodies. Arrows indicate cortactin localization at lamellipodia. (E) Equal amounts of crude lysates of control and Alix knockdown WI38 cells were immunoblotted for each of the indicated proteins. (F) Control or Alix knockdown WI38 cells were lysed in the actin stabilization buffer and F-actin in crude cell lysates were pelleted by ultracentrifugation. Proteins in the supernatants (lane S) and pellets (lane P) were immunoblotted with anti-cortactin antibodies (upper panel). After relative amounts of cortactin in the paired samples were determined, the percentage of cortactin in the pellet fraction (P) was calculated for control and Alix knockdown cells, respectively.

Figure 7 shows that Alix interacts with α-actinin and promotes α-actinin association with F-actin. (A) WI38 cell lysates were immunoprecipitated with 3A9 or anti-α-actinin antibodies, and the immunoprecipitates were immunoblotted for both Alix and α-actinin. (B) WI38 cell lysates were incubated with GST or GST-Alix fusion proteins illustrated in Fig. 6C, and bound proteins were immunoblotted with anti-α-actinin antibodies. (C) Equal amounts of crude lysates of control and Alix knockdown WI38 cells were immunoblotted for each of the indicated proteins. (D) Control or Alix knockdown (-) WI38 cells were lysed in the actin stabilization buffer and F-actin in crude cell lysates were pelleted by ultracentrifugation. Proteins in the supernatants (lane S) and pellets (lane P) were immunoblotted with anti-α-actinin antibodies (upper panel). After the relative amounts of α-actinin in the paired two fractions were determined, the percentage of α-actinin recovered in the pellet fraction (P) was calculated for control and Alix knockdown cells, respectively. (E) Control or Alix knockdown WI38 cells were

immunostained with anti-α-actinin antibodies. Arrows indicate aggregates of α-actinin in Alix knockdown cells.

Figure 8 shows a schematic illustration of conserved domains in Alix and regions in Alix that bind F-actin or F-actin binding proteins. The conserved domains of Alix and docking sites/regions for previously identified binding partners of Alix (on the top) and actin cytoskeleton proteins (at the bottom) are illustrated.

Figure 9 shows that Alix is present in the culture substratum. WI38 cells were transfected with control or Alix-specific siRNA. 24 hrs after the transfection, cells were re-plated on glass coverslips and cultured for 48 hrs. (A) Total proteins were extracted and immunoblotted with anti-Alix antibodies and anti-actin antibodies. (B) Cells were fixed with 4% paraformaldehyde and immunostained with 1A12 (green) by indirect immunofluorescence and counterstained with the DNA dye propidium iodide (red). Lower panels show enlarged images of the indicated areas in the upper panels. Arrows indicate staining of the substratum by 1A12 antibody.

Figure 10 shows that the 3A9 antibody preferentially stains substratum and cell periphery by immunogold electron microscopy. (A, B & C) Monolayer cultures of WI38 cells were immunogold-labeled with 3A9 antibody and the embedded samples were sectioned sagittally or horizontally and examined by electron microscopy. (A) An electron micrograph of a sagittal cell section shows preferential staining of substratum (arrows) and cell surface (arrowheads) by 3A9 antibody. (B) An electron micrograph of a horizontal cell section shows staining of clusters on the cell surface and in the area beneath the plasma membrane (arrowheads) by 3A9 antibody. (C) An electron micrograph of a horizontal cell section shows concentrated staining of membrane protrusion areas (arrow) by 3A9 antibody. (D) Monolayer cultures of WI38 cells were fixed with EM fixative (see text) and stained with 3A9 antibody or mouse IgG (mIgG) followed by FITC-conjugated secondary antibodies. Arrows indicate staining of the substratum or particles/clumps at the cell periphery.

Figure 11 shows that full-length Alix is present in the substratum. (A) After live WI38 cells were incubated with each of the indicated antibodies, cells were fixed, permeabilized and stained with FITC-conjugated secondary antibodies (green) and TRITC-conjugated phalloidin (red). Arrows show particular staining in the substratum. (B) Protein extracts of non-biotinylated

or biotinylated WI38 cell cultures were immunoprecipitated with anti-Alix antibodies or mouse IgG, and starting materials and immunoprecipitates were immunoblotted with anti-Alix antibodies (left panel) and streptavidin as indicated. (C) After WI38 cells were dissociated from monolayer cultures by EGTA, proteins were extracted from collected cells and remaining substratum separately, and equivalent percentages of samples were immunoblotted with anti-Alix antibodies.

Figure 12 shows that full-length Alix is present on the cell surface. (A&B) Live WI38 cells in suspension were incubated with the indicated antibodies for 1 hr at 4°C, and cells were washed with PBS to eliminate non-bound antibodies. (A) Cells were fixed and double stained with FITC-conjugated anti-mouse IgG (green) and propidium iodide (red). Arrows show staining of Alix on the cell surface. (B) After cells were lysed, cell lysates were incubated with protein G agarose and bound proteins were immunoblotted with anti-Alix antibodies. (C) After live WI38 cells in suspension were biotinylated, crude lysates of these cells were immunoprecipitated with anti-Alix antibodies or mouse IgG, and immunoprecipitates were immunoblotted with anti-Alix antibodies or streptavidin as indicated.

Figure 13 shows that full-length Alix is present in conditioned medium. (A) Conditioned medium collected from WI38 cell cultures was fractionated into designated fractions by consecutive centrifugation (see methods), and total proteins were extracted from remaining cells on the plate. Total proteins from medium fractions and 1/10 of the crude cell lysates from the same culture were immunoblotted in parallel with anti-Alix antibodies. P: pellet. SN: Supernatant. (B) Protein extracts of the 100,000 g pellet fraction (upper panel) and crude cell lysates (lower panel) were fractionated by gel filtration through Superose 6, and the proteins in the indicated fractions were precipitated with TCA and immunoblotted with anti-Alix antibodies.

Figure 14 shows that Anti-Alix antibodies inhibit integrin-mediated cell adhesion. (A) Live WI38 cells in suspension were incubated with each of the indicated antibodies at 4°C for 1 hr and then seeded in the continued presence of the antibody. At 1 hr after cell seeding, relative numbers of attached cells were determined and normalized. (B) Control or Alix knockdown WI38 cells in suspension were incubated with 1A12 antibody or mouse IgG (mIgG) at 4 °C for 1 hr and then seeded in the continued presence of the antibody. At 1 hr after cell seeding, relative

numbers of attached cells were determined and normalized. Crude lysates of control or Alix knockdown cells were immunoblotted with anti-Alix and anti-actin antibodies (right panel). (C) Live WI38 cells in suspension were incubated with 1A12 antibody or mouse IgG (mIgG) at 4°C for 1 hr and then seeded onto the substratum that was pre-coated with fibronectin (FN), vitronectin (VN), collagen (CN), or poly-L-lysine (PLL) in the continued presence of the antibody. At 1 hr after seeding, relative numbers of the attached cells were determined. Note: results in (A) and (B) are average from three independent experiments and the error bars show the standard error of mean (SEM) Results in (C) are obtained from a representative experiment out of three. Error bars show standard deviation. (D) Live WI38 cells in suspension were incubated with 1A12 antibody or mouse IgG (mIgG) at 4°C for 1 hr and seeded onto the substratum that was pre-coated with vitronectin in continued presence of the antibody. At 1 hr after cell seeding, cells were stained with crystal violet and photographed.

Figure 15 shows that extracellular Alix inhibits αvβ3 integrin-mediated cell adhesion. (A) After control (C) or Alix knockdown (-) WI38 cells were biotinylated, crude lysates of these cells were immunoprecipitated with anti-$\alpha_v\beta_3$ or anti-$\alpha_5\beta_1$ integrin antibodies. The immunoprecipitates were blotted with streptavidin. Star shows the ~95 kDa polypeptide in $\alpha_v\beta_3$ immunoprecipitates. (B) Crude lysates from monolayer culture of WI38 cells were immunoprecipitated with anti-$\alpha_v\beta_3$ integrin antibody and the immunoprecipitates were immunoblotted with anti-Alix antibodies. Star shows the slow-migrating isoform of Alix. (C) Control or Alix knockdown (-) WI38 cells were trypsinzied and incubated with anti-$\alpha_v\beta_3$, anti-$\alpha_5\beta_1$ integrin antibodies or control IgG at 4°C for 1 hr before seeding to regular culture dishes. At 1 hr after cell seeding, the numbers of attached cells were counted and the percentage of attached cells in the presence of anti-integrin antibodies as compared to those in the presence of control antibodies was calculated. Error bars show standard deviation of triplet dishes. (D) Control or Alix knockdown WI38 cells were trypsinzed and re-plated on fibronectin-coated glass coverslips for 1 hr. Cells were then fixed and immunostained with anti-$\alpha_v\beta_3$ or anti-$\alpha_5\beta_1$ integrin antibodies as indicated. Arrows point at the $\alpha_v\beta_3$ integrin-positive focal adhesions. Arrowheads point at the $\alpha_5\beta_1$ integrin-positive adhesions at either the center or the periphery areas.

Figure 16 shows Alix on Hela cell surface.

Figure 17 shows Alix on Hela cell surface.

Figure 18 shows Alix on Hela cell periplasm.

The patent or application file contains at least one drawing executed in color. Copies of this patent or patent application publication with color drawing(s) will be provided by the Office upon request and payment of the necessary fee.

While the present disclosure is susceptible to various modifications and alternative forms, specific example embodiments have been shown in the figures and are described in more detail below. It should be understood, however, that the description of specific example embodiments is not intended to limit the invention to the particular forms disclosed, but on the contrary, this disclosure is to cover all modifications and equivalents as illustrated, in part, by the appended claims.

DESCRIPTION

The present disclosure, according to specific example embodiments, generally relates to production and methods of use of antibodies. In particular, the present disclosure relates to anti-Alix antibodies and associated methods of using such antibodies in studies relating to Alix, including but not limited to properties such as the structure, function, and distribution of Alix in cells or in a suspension. In order to appreciate the utility of these anti-Alix antibodies, a detailed description of the structure and function of Alix is appropriate.

Alix in Actin Cytoskeleton Assembly

Normal fibroblasts grow as a single layer, assume flattened and elongated cell shape and align in parallel in monolayer culture. These morphological properties are determined by coordinated actin cytoskeleton assembly, integrin-mediated cell adhesion and extracellular matrix assembly (48). Filamentous-actin (F-actin) based structures, such as lamellipodia and filopodia at the leading edge of the cell and actin bundles in the central and peripheral regions of the cell body are assembled adjacent to the plasma membrane and anchored to extracellular matrix through integrin-mediated cell adhesions (1-4). Disregulation of any of these processes may cause alterations in fibroblast morphology, as often observed in transformed fibroblasts (5-

7). Critical regulators of these processes are often identified by their ability to alter fibroblast morphology when their expression levels are increased or decreased.

Alix/AIP1 (ALG-2 interacting protein X or 1) is the mammalian ortholog of an evolutionally conserved family of adaptor proteins (8). Our investigation of biological functions of human Alix, which was originally identified by us and named Hp95 (79, 80), has revealed its critical roles in regulating fibroblast morphology. In immortalized mouse fibroblast NIH/3T3 cells that are less flattened and aligned than their non-immortalized counterparts, overexpression of Alix promoted cell flattening and alignment, whereas reduction of Alix expression produced opposite effects (80). Alix overexpression also promoted cell flattening and monolayer growth in malignant HeLa cells (79). Since cell morphology is determined by coordinated actin cytoskeleton assembly, integrin-mediated cell adhesions and extracellular matrix assembly, these findings indicate that Alix plays structural or regulatory roles in some of these processes.

Functional studies of Alix and its orthologs have generated the consensus that Alix is positively involved in apoptotic induction (8, 9, 74, 80) and sorting of endocytosed cell surface receptors into the luminal vesicle of multivesicular bodies (MVB), also called late endosomes (10, 11, 61). Structurally, Alix and its orthologs are characterized by an N-terminal Bro1 domain, a middle region and a C-terminal proline-rich domain (PRD). The Bro1 domain, named after the first identified ortholog of this family, yeast Bro1, was originally predicted by computer program-based sequence analysis and thought to consist of the N-terminal 160 amino acid residues. Recent X-ray crystallography of bacterially produced fragments of Bro1 suggested that the N-terminal 380 residues (called broad Bro1 domain) are required to form a structurally stable domain for partner protein interaction (12). The middle region contains coiled-coil motifs, potential sites for additional partner protein interaction (10). The PRD contains multiple poly-proline motifs, which are potential docking sites for proteins containing SH3 domains. The apoptotic function of Alix requires its interaction with the calcium binding protein ALG-2 at the PRD (13, 14, 58, 74). The role of Alix in endosomal sorting requires binding the ESCRT-III component CHMP4b at the broad Bro1 domain and the ESCRT-I component TSG101 at the PRD (52, 71, 76). These functions of Alix do not seem to link to the effect of Alix on fibroblast morphology. Besides these well-established functions of Alix, Alix co-immunoprecipitated with

EGFR, multiple cytoskeletal proteins including actin and focal adhesion kinases in crude lysates of rat astrocytes (68). Although the physical nature or the functional implication of these associations was not determined in this study, these observations raised the possibility that Alix is a component of the transmembrane protein network that orchestrates coordinated actin cytoskeleton assembly, integrin-mediated cell adhesions and extracellular matrix assembly. To explore this possibility, we used non-immortalized WI38 cells derived from human lung fibroblasts as the model system to determine where in the transmembrane protein network Alix performs functions that regulate cell morphology. Experimental findings disclosed herein show that Alix associates with actin cytoskeleton and promotes its assembly.

We previously demonstrated that Alix promotes cell flattening and alignment in immortalized NIH/3T3 cells (80). This study made the first attempt to dissect the mechanism by which Alix regulates cell morphology. Using non-transformed WI38 cells as the model system, which requires Alix expression for maintenance of typical fibroblast morphology, we have discovered that Alix associates with both F-actin and F-actin based structures, including lamellipodia and stress fibers. Dramatically reducing Alix expression by siRNA both decreases F-actin content and inhibits F-actin assembly into higher order structures. In addition, recombinant Alix interacts with F-actin in a dose-dependent and stoichiometric manner in cell free system, and actin is the most abundant partner protein of Alix in WI38 cell lysates. Recombinant Alix also independently binds cortactin, which activates the ARP2/3 complex-mediated initiation of actin polymerization, and α-actinin, a key factor that bundles F-actin in stress fibers. Alix knockdown reduces the amount of cortactin and α-actinin in the F-actin fraction and abolishes lamellipodial localization of cortactin. These findings establish direct involvement of Alix in actin cytoskeleton assembly and uncovered at least one of the major mechanisms by which Alix regulates fibroblast morphology. Moreover, our findings offer a plausible explanation for the recent observation that Alix knockdown in HeLa cells caused an abnormal distribution of endosomes and the cortical proteins involved in endocytosis such as clathrin and cortactin (28).

Alix knockdown consistently reduces the overall cell staining by phalloidin, which stains both distinct F-actin based structures such as lamellipodia and stress fibers and "amorphous" F-

actin meshworks and scattered F-actin in the cytoplasm (21-24) (Fig. 3B). This indicates that Alix plays positive roles in actin polymerization or stability. Previous studies have established that actin polymerization is nucleated at lamellipodial protrusions or endosomes by membrane associated Arp2/3 complex (30). Cortactin binds the Arp2/3 complex and activates the Arp2/3 complex-mediated actin polymerization. This process not only drives lamellipodial protrusions at the plasma membrane and directional movement of endosomes in the cytoplasm (27), but also determines the abundance of F-actin that can be assembled into stress fibers and other types of F-actin based structures (31, 32). Based on these previous findings, the inhibitory effect of Alix knockdown on lamellipodial localization of cortactin may explain or contribute to the negative effects on both F-actin content.

In addition to reduced F-actin content, Alix knockdown cells also formed fewer and shorter stress fibers, especially in the central region of the cells (Fig. 3D). Although this abnormality can be simply attributed to the reducing effect of Alix knockdown on the F-actin content, Alix localization at stress fibers and Alix association with the F-actin bundling protein α-actinin raise the possibility that Alix has an independent function in stress fiber assembly. Previous studies have established that key steps in stress fiber assembly are bundling of F-actin by α-actinin and association with F-actin bundles with myosin-bundles (39). Since Alix directly interacts with α-actinin and promotes its association with F-actin, Alix may play a positive role in the F-actin bundling step in stress fiber assembly.

Alix has been implicated in diverse cellular processes by binding a variety of partner proteins. However, none of these previous studies examined the relative abundance of these proteins in the Alix complexes in any cell systems or provided quantitative information on partition of Alix to different structures or functions. In this study, we performed the first proteomic analysis of the components in the Alix complex in mammalian cells lysates and obtained evidence that actin is a major Alix binding partner in WI38 cells. This was consistent with co-localization of the majority of the Alix staining with F-actin staining in WI38 cells. These findings indicate that regulation of actin cytoskeleton assembly is a major biological function of Alix in mammalian fibroblasts.

The yeast ortholog of Alix, Bro1, was originally identified by mutations causing increased osmotic sensitivity. In addition to this defect, the mutant cells showed larger sizes and abnormal cell shapes (33). However, neither the characterized roles of Bro1 in endosomal trafficking nor other known functions of Bro1 or related proteins account for these morphological defects. Since proper assembly of cortical cytoskeleton by F-actin cross-linking proteins has been demonstrated to protect yeast cells from osmotic stress and insure normal cell sizes and shapes (34), it is conceivable that the role of Alix in regulating the actin cytoskeleton is evolutionally conserved and that Bro1 mutation generates these mutant phenotypes through causing defects in the actin-cytoskeleton.

Alix is structurally characterized by an N-terminal Bro1 domain, a middle region and a C-terminal PRD (61). As illustrated in Fig. 8, previous studies have established that the PRD interacts with multiple cellular Alix binding partners that are involved in apoptotic induction (ALG-2), endosomal sorting (TSG-101) and endocytosis (SETA/CIN85) (14, 71, 76, 42). A short region adjacent to the PRD interacts with two viral proteins (P6 and P9) (71). Moreover, the recently defined broad Bro1 domain, which includes both the Bro1 domain and the C-terminal 200 residues, interacts with CHMP4b also involved in endosomal sorting (12). In this study, we have demonstrated that both the Bro1 domain and the PRD bind F-actin.

This is the first example that the structurally conserved Bro1 domain actually interacts with a partner protein. The N-terminal half of the middle region of Alix interacts with α-actinin. The C-terminal half of the middle region of Alix contains a docking site for cortactin, which localizes before the region that interacts with the two viral proteins. The involvement of all major regions of Alix in its interaction with actin cytoskeleton proteins predicts that the role of Alix in actin cytoskeleton assembly involves the whole molecule and that a truncated Alix may have dominant negative effects on the role of Alix in actin cytoskeleton assembly. Consistent with this possibility, the Alix-related protein rhophilin, which contains an intact Bro1 domain but lacks a counterpart of the middle region or the PRD of Alix (35, 64), was previously shown to inhibit stress fiber assembly in a Bro1 domain-dependent manner (64).

Extracellular Alix and Its Roles in Modulating Integrin-Mediated Cell Adhesions

Alix/AIP1 (ALG-2 interacting protein X or 1) is the mammalian ortholog of an evolutionally conserved family of adaptor proteins. These proteins are characterized by an N-terminal Bro1 domain and a C-terminal proline-rich domain (PRD), both of which mediate protein-protein interactions (8). Previous studies have demonstrated that Alix interacts with a variety of cytoplasmic proteins in addition to the EF-hand calcium binding protein ALG-2, including the ubiquitin ligase-like protein TSG-101 (76), the endosomal membrane-associated protein CHMP4b (51, 52), the lysophosphatidic acid acyltransferase endophillin (41), the SH3-domian containing protein CIN85/SETA (42). Alix interactions with these partner proteins regulate apoptotic signaling (58, 74), endocytosis (69) or multivesicular body (MVB) sorting of endocytosed transmembrane proteins (53, 61, 76). Consistently, Alix has been localized to the soluble and membrane-associated fractions of the cytoplasm by both biochemical and immunological approaches (41, 42, 74).

Several reasons made us speculate that the positive role of Alix in actin cytoskeleton assembly may not be the only function that Alix performs in the transmembrane network that regulates cell morphology. In addition to Alix orthologs that have been identified from yeast to human, Alix-related proteins that lack the C-terminal PRD also exist in lower eukaryotes (40, 81). Interestingly, one such protein in the parasite *E. histolytica*, called adhesin, is present on the extracellular side of the plasma membrane and is functionally important for heterophilic cell-cell adhesion and phagocytosis with undefined mechanisms (47). The 76-kDa adhesin covalently links to a cysteine protease, forming a chimera protein of 112 kDa (47). Antibodies that recognize the adhesin portion of the chimera protein inhibited adherence of the parasite to target cells and the subsequent phagocytosis (46, 47). The cysteine protease portion of the 112-kDa protein contains an RGD sequence for potential interaction with integrin (38). Although mammalian cells do not contain an independent adhesin ortholog in the database, the presence within Alix of an ortholog of adhesin raises a formal possibility that Alix may perform extracellular functions that regulate cell adhesions in addition to its various cytoplasmic functions. Consistent with this possibility, we consistently observed above-background staining of the substratum of WI38 cell cultures by certain anti-Alix antibodies. Also, the morphological defects of Alix-knockdown WI38 cells were more severe after subculture (62), which could not

be satisfactorily explained by the intracellular roles of Alix in actin cytoskeleton assembly. We therefore designed a study to explore the extracellular allocation and function of Alix using WI38 cells as the model system.

Alix and its orthologs in other species have always been considered cytoplasmic proteins. Although Alix has been detected as a component of exosomes from dendritic cells (73) and HIV-1 viral particles (71), it has never been suspected that Alix may localize at the extracellular side of the plasma membrane. Thus, this study is the first effort that investigates the extracellular allocation and function of Alix or any of its orthologs. Our data show that Alix is present in extracellular compartments and that the extracellular Alix has functions in regulating cell adhesions. These findings place Alix into the special category of eukaryotic proteins that functions both intracellularly and extracellularly (60).

Extracellular distribution of Alix

We previously generated multiple anti-Alix monoclonal antibodies and examined the sub-cellular localization of Alix in WI38 cells. The results clearly demonstrated that Alix is an abundant cytoplasmic protein that localizes at various actin-based cytoskeletal structures (62). In this study, we demonstrated that, although predominantly cytoplasmic, Alix is present in all of the three extracellular compartments of WI38 cell cultures, i.e., the substratum, cell surface and conditioned medium. Moreover, the extracellular Alix differs from the predominant intracellular Alix in biochemical and/or immunological properties. The predominant intracellular Alix is ~150 kDa by gel filtration, cannot be stained by 1A12 and 3A9 antibodies under cell fixation for EM and often contains cleavage products. In contrast to the predominant intracellular Alix, Alix in the conditioned medium is ~5000 kDa by gel filtration. Alix on the cell surface and in the substratum can be readily recognized by 1A12 and 3A9 antibodies under the EM fixation condition. In none of the three extracellular compartments were cleaved products of Alix readily detected. Since Alix with such distinct properties cannot be accounted for by the negligible level of cell lysis observed in WI38 cell cultures, these findings indicate that WI38 cells actively transport a special population(s) of Alix from the cytoplasm to extracellular compartment. Consistent with this conclusion, the immunologically distinct Alix exists not only on the cell surface but also in the area beneath the plasma membrane, indicating their intracellular origin.

Our finding of extracellular allocation of Alix has several potential implications. First of all, it raises the issue of which of the biological functions of Alix or its orthlogs are carried out by the extracellular Alix and which by the intracellular Alix. For example, Alix that associates with exosomes from dendritic cells has been implicated in processes related to apoptosis. This speculation was based on the defined role of the intracellular Alix in apoptotic induction (58, 74). However, if Alix localizes not within the exosomes as it was originally assumed but actually on the surface of the exosome membrane, potential roles that the exosome Alix plays may be very different. Another example is that Alix overexpression was shown to inhibit cell adhesions in HEK293 cells by electrical cell-substrate impendence sensor (ECIS) assay. This effect of Alix was thought to be due to its ability to associate with focal adhesion kinases and inhibit their kinase activities (68). Since we now know that the extracellular Alix could also inhibit cell adhesion, the effects of Alix overexpression on cell adhesion might be a combination of both intracellular and extracellular functions of Alix. Another potential implication of our findings is on Alix regulation. Export of only a small portion of Alix across the plasma membrane implies presence of the regulatory mechanism that controls the amount of the protein to be exported and the balance between the intracellular and extracellular functions of Alix. Our preliminary results showed that transformed cells secrete more Alix into the conditioned medium (unpublished results). In this context, the difference in the immunological and biochemical properties of the intracellular and extracellular Alix indicate that these two populations of Alix exist in different conformations and raise the possibility that protein modification may be an important step for the cytoplasmic Alix to become exportable.

How the cytoplasmic Alix is transported to the extracellular side of the plasma membrane is yet to be understood. We did not detect inhibitory effects of monensin or brefeldin A, the inhibitors of the ER/Golgi-dependent pathway (44, 65), on secretion of Alix to the culture medium (data not shown), making it unlikely that Alix is exported through the ER/Golgi-mediated vesicle transport system. Although Alix is involved in late endosome trafficking, Alix localizes at the cytoplasmic side of the endosome membrane through its association with ESCRT I and III complexes (52, 64, 76). Besides these common mechanisms that may export proteins, it has been reported that cytoplasmic proteins may export across the plasma membrane through a

process called ectocytosis, which involves formation of protein aggregates underneath the plasma membrane and inclusion of the protein aggregates into plasma membrane blebbings (56, 70). Since Alix at the cell periphery often exists in clustered forms as revealed by immuno-gold electron microscopy, it is possible that Alix is exported through this mechanism.

Extracellular functions of Alix

Majority of proteins in extracellular compartments of mammalian cultured cells play structural or regulatory roles in cell adhesion or extracellular matrix assembly (50, 59). Since the Alix-related protein adhesin is already known to be involved in heterophilic cell-cell adhesion, we focused our attention on the potential role of Alix in cell adhesions. We found that perturbation of the extracellular Alix by 3A9 and 1A12 anti-Alix antibodies severely inhibited attachment and spreading of WI38 cells on the extracellular matrix proteins vitronectin and fibronectin. This was reminiscent of the previous finding that antibodies that recognized the adhesin inhibited adhesion of trophozoites to target cells (55). Interestingly, both 1A12 and 3A9 antibodies recognize epitopes that localize in between residues 607-709 of Alix (82). This region of Alix overlaps with the region in adhesin that is recognized b the inhibitory antibodies (39, 55). Moreover, the extracellular Alix co-immunoprecipitated with α_V/β_3 integrin, which binds both vitronectin and fibronectin. These findings indicate that Alix on the cell surface is physically linked to α_V/β_3 integrin. By reducing the level of Alix expression by siRNA, we found that Alix knockdown enhanced α_V/β_3 integrin-mediated cell adhesion. This finding qualified Alix as a negative regulator of α_V/β_3 integrin-mediated cell adhesion although it alone could not distinguish whether the effect was achieved through the intracellular or extracellular Alix. However, in conjunction with the physical linkage of the extracellular Alix to α_V/β_3 integrin and positive effects of the intracellular Alix on actin cytoskeleton assembly and focal adhesion kinases (62), which are unlikely to suppress α_V/β_3 integrin-mediated cell adhesion, the most plausible explanation for this finding is that the extracellular Alix is a negative regulator of α_V/β_3 integrin-mediated cell adhesion.

How the extracellular Alix binds α_V/β_3 integrin and why it inhibits α_V/β_3 integrin-mediated cell adhesion are yet to be understood. One class of extracellular proteins that interact

with α_V/β_3 integrin, including vitronectin, fibronectin, fibrinogen and thrombospondin, contain an RGD sequence that directly binds α_V/β_3 integrin (72). Since Alix does not contain an RGD motif (data not shown), it is unlikely that Alix inhibits α_V/β_3 integrin-mediated cell adhesion by occupying the RGD binding site in α_V/β_3 integrin. However, the Alix-related protein adhesin covalently links to a protein that contains an RGD sequence (47). Although Alix does not covalently link to another protein, Alix contains a C-terminal PRD that is absent in adhesin. The PRD contains multiple docking sites for binding partners (8), allowing Alix to be physically linked to other proteins in a non-covalent manner. Thus it is possible that Alix on the cell surface binds to a protein that contains an RGD sequence, and this RGD sequence may compete with the RGD sequence in α_V/β_3 integrin ligand for binding and thus inhibit the ability of α_V/β_3 integrin to assemble cell adhesion complexes. Although this is an attractive working hypothesis that will be tested in our future studies, we are aware that this is not the only plausible explanation that may account for the negative effect of the extracellular Alix on α_V/β_3 integrin-mediated cell adhesion. There are extracellular proteins that interact with α_V/β_3 integrin through non-RGD motifs and modulate α_V/β_3 integrin functions through changing its conformations (37, 77, 78). Thus it is also possible that the extracellular Alix directly binds α_V/β_3 integrin and links it to proteins that may affect the integrin conformation. In any event, our findings have opened a new ground in the field of outside-in regulation of integrin function (49).

Besides inhibiting α_V/β_3 integrin-mediated cell adhesion, the extracellular Alix may also modulate α_5/β_1 integrin-mediated cell adhesion through a different mechanism. We found that antibody binding to the extracellular Alix greatly inhibited attachment of WI38 cells not only to vitronectin, but also to fibronectin (Figure 13C). Since α_V/β_3 integrin not only is the primary receptor for fibronectin (67), but also plays more important roles than α_V/β_3 integrin in attachment of WI38 cells to the substratum (Figure 14C), the observed inhibition of cell attachment to fibronectin by antibody perturbation of the extracellular Alix was hard to be accounted by the inhibitory effect on α_V/β_3 integrin alone and probably also involved the effect on α_5/β_1 integrin. However, antibody binding to the extracellular Alix inhibited spreading of WI38 cells on fibronectin to a lesser extent than on vitronectin. Alix did not co-

immunoprecipitate with α_5/β_1 integrin. Moreover, reducing Alix expression clearly and reproducibly inhibited centripetal translocation of α_5/β_1 integrin and formation of fibrillar adhesion but did not promote the overall formation of α_5/β_1 integrin-mediated cell adhesion as it did to α_V/β_3 integrin-mediated cell adhesion (Figure 14C&D). These findings indicated that the effect of the extracellular Alix on α_5/β_1 integrin-mediated cell adhesion is different from that on α_V/β_3 integrin-mediated cell adhesion.

Coordinated formation of the static α_V/β_3 integrin-mediated cell adhesion and dynamic α_5/β_1 integrin-mediated cell adhesion play instrumental roles in fibroblast morphology (43). Since Alix in the extracellular compartment regulates both α_V/β_3 and α_5/β_1 integrin-mediated cell adhesions, it is reasonable to speculate that, in addition to the positive role of the intracellular Alix in actin cytoskeleton assembly (62), the extracellular function of Alix also contributes to the critical role of Alix in maintenance of fibroblast morphology.

Anti-Alix Antibodies

The present disclosure describes antibodies that bind Alix protein in cells. Several variants of these anti-Alix antibodies are disclosed herein, including 3A9 and 1A12. Most of the prior anti-Alix antibodies have low efficiencies in recognizing Alix using immunoblotting. None of the existing antibodies are able to recognize non-denatured Alix in crude cell lysates or in the cells after fixation. 3A9 is the first anti-Alix antibody that recognize both denatured and non-denatured Alix with high efficiency. Since Alix is involved in apoptosis, vesicle trafficking, virus budding, this antibody will be a great tool in uncovering the exact functions of Alix in these cellular processes. 1A12 and 3A9 antibodies are the only available anti-Alix antibodies that are able to label this subpopulation of Alix in live cell cultures and inhibit integrinmediated cell adhesions. The 1A12 antibody is more consistent and efficient than 3A9 antibody in these types of the assays.

According to the disclosure, GST-Alix polypeptides produced recombinantly or by chemical synthesis, and fragments or other derivatives, may be used as an immunogen to generate antibodies that recognize the GST-Alix polypeptide or portions thereof. Such antibodies include, but are not limited to, polyclonal, monoclonal, humanized, primatized, chimeric, single

chain, Fab fragments, and a Fab expression library. An antibody that is specific for human Alix protein may recognize a wild-type or mutant form of Alix protein. In particular embodiments, antibodies are produced to, but not limited to, Alix proteins, and variants thereof. Specific examples of such antibodies include, but are not limited to, antibodies that are capable of binding to Alix surface protein products from various regions of the Alix protein.

Various procedures known in the art may be used for the production of polyclonal antibodies to polypeptides, derivatives, or analogs. For the production of antibody, various host animals, including but not limited to rabbits, mice, rats, sheep, goats, etc, can be immunized by injection with the polypeptide or a derivative (e.g., fragment or fusion protein). The polypeptide or fragment thereof can be conjugated to an immunogenic carrier, e.g., bovine serum albumin (BSA) or keyhole limpet hemocyanin (KLH). Various adjuvants may be used to increase the immunological response, depending on the host species, including but not limited to Freund's (complete and incomplete), mineral gels such as aluminum hydroxide, surface active substances such as lysolecithin, pluronic polyols, polyanions, peptides, oil emulsions, KLH, dinitrophenol, and potentially useful human adjuvants such as BCG (bacille Calmette-Guerin) and Corynebacterium parvum.

Monoclonal antibodies directed toward an Alix polypeptide, fragment, analog, or derivative thereof, may be prepared by any technique that provides for the production of antibody molecules by continuous cell lines in culture may be used. These include but are not limited to the hybridoma technique originally developed by Kohler and Milstein *Nature* 256:495-497, 1975), as well as the trioma technique, the human B-cell hybridoma technique (Kozbor et al., *Immunology Today* 4:72, 1983; Cote et al., *Proc. Natl. Acad. Sci. U.S.A.* 80:2026-2030, 1983), and the EBV-hybridoma technique to produce human monoclonal antibodies (Cole et al., in Monoclonal Antibodies and Cancer Therapy, Alan R. Liss, Inc., pp. 77-96, 1985). Accordingly, the present disclosure is also directed to hybridoma cell lines that produce a monoclonal antibody that specifically binds to an antigen (e.g., Alix protein).

Additionally, "Chimeric antibodies" may be produced (Morrison et al., *J. Bacteriol.* 159:870, 1984; Neuberger et al., *Nature* 312:604-608, 1984; Takeda et al., *Nature* 314:452-454, 1985) by splicing the genes from a non-human antibody molecule specific for a polypeptide

together with genes from a human antibody molecule of appropriate biological activity. For example, a chimeric antibody, wherein the antigen-binding site is joined to human Fc region, e.g., IgG1, may be used to promote antibody-dependent mediated cytotoxicity or complement-mediated cytotoxicity. In addition, recombinant techniques known in the art can be used to construct bispecific antibodies wherein one of the binding specificities is that of an antibody of the present disclosure (*See, e.g.*, U.S. Pat. No. 4,474,893).

According to the present disclosure, techniques described for the production of single chain antibodies (U.S. Pat. Nos. 5,476,786; 5,132,405; and 4,946,778) can be adapted to produce HERV-K *env* protein antigen-specific single chain antibodies. An additional embodiment of the disclosure utilizes the techniques described for the construction of Fab expression libraries (Huse et al., *Science,* 246:1275-1281, 1989) to allow the rapid and easy identification of monoclonal Fab fragments with the desired specificity, or fragment derivatives, or analogs.

Antibody fragments which contain the idiotype of the antibody molecule can also be generated by known techniques. For example, such fragments include, but are not limited to, the $F(ab')_2$ fragment which can be produced by pepsin digestion of the antibody molecule; the Fab′ fragments which can be generated by reducing the disulfide bridges of the $F(ab')_2$ fragment, and the Fab fragments which can be generated by treating the antibody molecule with papain and a reducing agent. Anti-idiotypic monoclonal antibodies to the antibodies of the present disclosure are also contemplated.

In the production and use of antibodies, screening for or testing with the desired antibody can be accomplished by techniques known in the art, e.g., radioimmunoassay, ELISA (enzyme-linked immunosorbant assay), "sandwich" immunoassays, immunoradiometric assays, gel diffusion precipitin reactions, immunodiffusion assays, in situ immunoassays (using colloidal gold, enzyme or radioisotope labels, for example), western blots, precipitation reactions, agglutination assays (e.g., gel agglutination assays, hemagglutination assays), complement fixation assays, immunofluorescence assays, protein A assays, and immunoelectrophoresis assays, etc.

In a specific embodiment, antibodies of the present disclosure are conjugated to a secondary component, such as, for example, a small molecule, polypeptide, or polynucleotide.

The conjugation may be produced through a chemical modification of the antibody, which conjugates the antibody to the secondary component. The conjugated antibody may allow for targeting of the secondary component, such as, for example, a cytotoxic agent or an anti-tumor agent or an imaging agent, to the site of interest. The secondary component may be of any size or length. Examples of secondary components include, but are not limited to, chemotherapeutic agents, toxins, photo-activated toxins (e.g., dihydropyridine- and omega-conotoxin), radioactive isotopes, mitotic inhibitors, cell-cycle regulators, and anti-microtubule disassembly compounds (e.g., taxol). For example, suitable cytotoxic agents include ricin A chain, abrin A chain, modeccin A chain, gelonin, melphalan, bleomycin, adriamycin, daunomycin, pokeweed antiviral proteins (PAP, PAPII, PAP-S), and granzyme B; and suitable anti-tumor agents include a lymphokine or oncostatin. In a specific embodiment, the secondary component is the toxin Gelonin (rGel), which is a potent inhibitor of cellular protein synthesis.

Those skilled in the art will realize that there are numerous radioisotopes and chemocytotoxic agents that can be coupled to tumor specific antibodies by well known techniques, and delivered to specifically destroy tumor tissue. *See, e.g.*, U.S. Pat. No. 4,542,225. Examples of imaging and cytotoxic reagents that can be used include ^{125}I, ^{111}In, ^{123}I, ^{99m}Tc, ^{32}P, ^{3}H, and ^{14}C; fluorescent labels such as fluorescein and rhodamine, and chemiluminescers such as luciferin. The antibody can be labeled with such reagents using techniques known in the art, for example, as described in Wenzel and Meares, *Radioimmunoimaging and Radioimmunotherapy*, Elsevier, N.Y. (1983) and Colcer et al., *Methods Enzymol.*, 121:802-16, 1986, and *Monoclonal Antibodies for Cancer Detection and Therapy*, Baldwin et al. (eds), pp. 303-16 (Academic Press 1985).

Other covalent and non-covalent modifications of the antibodies or antibody fragments of the present disclosure are embraced herein, including agents which are co-administered or administered after the antibody or fragments, to induce growth inhibition or killing of the cells to which the antibody or fragment has previously bound.

In another embodiment of the present disclosure, compositions are provided that comprise the monoclonal antibody, or antibody binding fragment as described herein, bound to a solid support. A solid support for use in the present disclosure will be inert to the reaction

conditions for binding. A solid phase support for use in the present disclosure must have reactive groups or activated groups in order to attach the monoclonal antibody or its binding partner thereto. In another embodiment, the solid phase support may be a useful chromatographic support, such as the carbohydrate polymers SEPHAROSE®, SEPHADEX®, or agarose. As used herein, a solid phase support is not limited to a specific type of support. Rather, a large number of supports are available and are known to one of ordinary skill in the art. Solid phase supports include, for example, silica gels, resins, derivatized plastic films, glass beads, cotton, plastic beads, alumina gels, magnetic beads, membranes (including, but not limited to, nitrocellulose, cellulose, nylon, and glass wool), plastic and glass dishes or wells, and the like.

Therefore, the present invention is well adapted to attain the ends and advantages mentioned as well as those that are inherent therein. While numerous changes may be made by those skilled in the art, such changes are encompassed within the spirit of this invention as illustrated, in part, by the appended claims.

EXAMPLES

Example 1

Production of recombinant proteins. cDNAs that encode full length and truncated Alix were generated by polymerase chain reaction (PCR) using the Alix cDNA clone obtained in previous studies as the template (79). PCR products were digested with BamH I and Not I restriction enzymes and inserted into the BamH I and Not I sites of the pGEX-4T3 vector (Amersham Biosciences, Piscataway, NJ). To express recombinant proteins from these cDNAs, BL-21 *E. coli* cells were transformed with produced cDNA constructs and induced at ~0.6 of OD600 with 0.1 mM IPTG at 37°C for 4 hrs. The induced cells were harvested by centrifugation at 5000 *g* for 10 min and re-suspended in phosphate-buffered saline (PBS) supplemented with 0.5% Triton X-100, 1 mM EDTA, 1 mM DTT, 0.35 M NaCl, 1 mM PMSF, 200 μg/ml lysozyme, 5 mM benzamidine (Sigma, St. Louis, MO) and 1 μg/ml each of leupeptin, pepstatin A, and chymostatin (Roche, Indianapolis, IN). The cells were then lysed by sonication, and the cell lysates were cleared by centrifugation at 13,000 *g* for 40 min. To purify the recombinant proteins, the cleared cell lysates were incubated with glutathione agarose (Sigma) overnight at 4°C on rotation. The resins were then column-washed with 20-bed volumes of 500 mM NaCl,

0.1 mM EDTA, 0.1 mM EGTA, 0.5% Triton X-100, 0.5% Tween-20 and 1 mM DTT in 50 mM Tris-HCl (pH 8.0). Following the wash, recombinant proteins on the beads were eluted with 10 mM reduced glutathione in PBS and stored in 20% glycerol at -70°C. To produce GST tagged Alix or Alix fragments by in vitro transcription and translation, cDNAs encoding these recombinnat proteins were amplified from their bacterial expression vectors by PCR with the forward primer 5'-ATTTAGGTGACACTATAGAAGCGAGCCACCATGGCCCCTATACTAGGTTATTG-3' and the reverse primer 5'-CCGGGAGCTGCATGTGTCAGAGGTTTTC-3'. These PCR products were transcribed directly using mMESSAGE mMACHINETM SP6 kit (Ambion, Austin, TX). Proteins were produced from the RNA products by in vitro translation using Retic lysates IVT kit (Ambion, Austin, TX).

Production and characterization of anti-Alix monoclonal antibodies. Balb/c mice were immunized with purified GST-Alix. Two weeks after immunization, blood samples were obtained from the tail of the immunized mice and tested for titers against GST-Alix by both ELISA and immunoblotting. Spleens from the mice that showed the highest titers were removed, and their splenocytes were fused with the mouse myeloma cell line SP2/0. Culture supernatants from individual hybridoma clones were then screened by ELISA and immunoblotting against GST-Alix. To produce antibodies from different hybridoma clones, the clones were seeded in stationary bioreactors in DMEM (BRL-Gibco, Grand Island, NY) plus 10% low-IgG fetal bovine serum from HyClone (Logan, Utah). The Bioreactor fluids were collected every 3 days, and IgG fractions were affinity-purified using protein G-agarose columns (Upstate Biotechnology, Lake Placid, NY). The concentrations of purified IgG were determined by their absorbance at OD_{280}.

Cell culture and transfection. WI38 cells, derived from human lung fibroblasts, were obtained from ATCC and cultured in regular culture dishes in Eagle's Minimal Essential Medium with Earle's Salts (Invitrogen, Carlsbad, CA) that was supplemented with 2 mM L-glutamine and 10% fetal bovine serum (Atlanta Biologicals, Lawrenceville, GA) unless otherwise indicated. WI38 cells were not immortalized and the 19^{th} to 30^{th} generations were used in this study. Two Alix-specific siRNAs and one green fluorescence protein (GFP)-specific siRNA were designed and synthesized by Dharmacon Research Inc. (Lafayette, CO). Alix-

specific siRNA sequences were 5'-gagaagaaattgcaaggtt-3'and 5'-gaaggatgctttcgataaa-3'. The GFP-specific siRNA sequence was 5'-ggctacgtccaggagcgcacc-3'. Transfection of siRNA was performed essentially as described previously (15). In brief, 2.5×10^5 WI38 cells were plated in 35-mm culture dishes and grown for 24 hrs. Each plate of cells was then transfected with 4 μl of 50 nM siRNA mixed with lipofectamine-2000 purchased from Invitrogen Corporation (Carlsbad, CA) following manufacturer's instruction. The transfected cells were either continuously cultured or subcultured at 24 hrs after the transfection at 10^4 cells per new dish. Cell morphologies were observed after 48 hrs and 72 hrs by phase contrast microscopy, and digital images were taken at 40× magnifications by Olympus IX81 microscope (Olympus America Inc. Melville, NY) using Metamorph software (Molecular Devices Corporation, Sunnyvale, CA).

Preparation of cell lysates, immuno-precipitation and immunoblotting. For testing the immunoblotting and immunoprecipitation efficiencies of anti-Alix antibodies, WI38 cells were scraped from culture dishes in ice-cold RIPA buffer (1% NP-40, 0.5% DOC, 0.1% SDS and 150 mM NaCl in 20 mM Tris-HCl, pH7.4) supplemented with 1 mM PMSF and 1 μg/ml each of leupeptin, pepstatin A and chymostatin (Roche) and incubated on ice for 30 min. For testing interactions between Alix and cortactin and α-actinin, WI38 cells were lysed by sonication in buffer containing 20mM Tris-HCl, 150mM NaCl, 5mM EDTA, 1mM PMSF, and 1 μg/ml each of leupeptin, pepstatin A and chymostatin. Collected cell lysates were centrifuged at 10,000 *g* for 30 min, and protein concentrations of supernatants were determined by using a DC protein assay kit purchased from Bio-Rad Laboratories (Hercules, CA). Immunoprecipitation of WI38 cell lysates was performed by incubation of 40 μl of crude cell lysates (~40 μg total proteins) with 2 μg of specific antibody immobilized onto 10 μl protein-G sepharose (Amersham Biosciences). The beads were then washed six times with 500 μl lysis buffer and were eluted by boiling in 5 bed volumes of SDS-PAGE sample buffer. The eluted proteins were resolved by 10% SDS-PAGE, transblotted onto nitrocellulose membrane and immunoblotted following the procedure as we previous described (16). Polyclonal anti-actin antibodies were purchased from Sigma Aldrich (St. Louis, MO). Polyclonal anti-cortactin and anti-myc antibodies, and monoclonal anti-

α-actinin and anti-CDK4 antibodies were purchased from Santa Cruz Biotechnology, Inc. (Santa Cruz, CA).

Immunofluorescence staining. WI38 cells were cultured on 22-mm glass coverslips placed in 35-mm culture dish. In some experiments, the glass coverslips were pre-coated at 4°C for overnight with 20 μg/ml fibronectin. After indicated time of culture, cells were fixed with 4% paraformaldehyde (Sigma), permeabilized with 0.5% Triton X-100 (Sigma) and blocked for 1 hr with 10% horse serum (Invitrogen) in PBS. Fixed cells were first incubated for 1 hr with 1 μg/ml of anti-Alix antibody diluted in 5% horse serum in PBS, followed by 3 times of wash with PBS/0.1% NP-40. Cells were then incubated for 1 hr with FITC-conjugated secondary antibody (Sigma) diluted 1:200 in 3% horse serum in PBS. After three times of wash, cells were mounted with anti-fade (Vector Laboratories, Burlingame, CA) and images were captured by the ZEISS Axioplan 2 imaging system (Carl Zeiss Microimaging Inc., Thornwood, NY) using Metamorph software (Molecular Devices Corporation). For co-staining with antibody and phalloidin, after the final wash, cells were incubated with 50 μg/ml phalloidin-TRITC (Sigma) in PBS for 30 min and rinsed in PBS before mounting. For immunofluorescence staining with two antibodies, a mixture of the two antibodies was used as primary antibody. FITC-conjugated anti-mouse IgG and Texas-red-conjugated anti-rabbit IgG (Vector laboratories) were used to detect monoclonal and polyclonal antibodies, respectively. For cytochalasin D treatment, WI38 cells were cultured on 22-mm glass coverslips for 24 hrs and the medium was replaced by fresh medium containing 5 μM of cytochalasin D (Sigma). After 30 min of incubation at 37°C, cells were washed 3 times with PBS. Cells were then fixed and stained with phalloidin-TRITC following the same procedure described above.

GST pull-down assays. 5 μg of purified GST or GST-tagged Alix or truncated Alix recombinant proteins were absorbed onto 5 μl glutathione-conjugated agarose beads (Sigma). The beads were then incubated at 4°C for 6 hrs with WI38 cell lysates (prepared in lysis buffer composed of 20 mM Tris-HCl, pH7.4, 150 mM NaCl, 5 mM EDTA, 1 mM PMSF and 1 μg/ml each of leupeptin, pepstatin A and chymostatin) containing ~ 50 μg of total proteins. The beads were washed eight times with the lysis buffer plus 0.5% NP-40 and eluted with 40 μl of SDS-

sample buffer. Eluted polypepetides were resolved by 10% SDS-PAGE, transblotted onto nitrocellulose membrane and immunoblotted with anti-cortactin or anti-α-actinin antibodies. To test Alix binding to G-actin, GST or GST-Alix absorbed glutathione agarose beads were incubated at 4°C overnight with 5 μg of purified non-muscle actin (Cytoskeleton, Denver, CO) dissolved in 40 μl of G-buffer (5 mM Tris-HCl, pH 8.0, 0.2 mM $CaCl_2$). The beads were washed eight times with G-buffer plus 0.5% NP-40 and 1 mM DTT and eluted with 40 μl of SDS-sample buffer. Eluted polypeptides were resolved in parallel with non-absorbed actin by 10% SDS-PAGE, transblotted onto nitrocellulose membrane and immunoblotted with anti-actin antibodies.

F-actin cosedimentation. F-actin co-sedimentation assay was performed on Alix in WI38 cell lysates or GST-Alix recombinant proteins using the Non-Muscle Actin Binding Protein Biochem Kit specifically designed for this assay (Cytoskeleton). All the samples were pre-cleared by centrifugation at 150,000 *g* for 1 hr before the assay. Quantitation of Coomassie blue stained polypeptides in the supernatant and pellet was performed by analyzing scanned images with NIH Image 1.62 as previously described (80). Data were analyzed by the curve fitting software PRIZM when indicated (ver. 3; GraphPad Software, San Diego, CA).

Separation of G-actin and F-actin in WI38 cell lysates. F-actin and G-actin in WI38 cell lysates was separated using a procedure described previously (17, 18). Briefly, WI38 cells were transfected with control or Alix siRNA. 48 hrs after transfection, cells were trypsinzed and 1×10^5 cells were re-plated into 35mm dishes and cultured for additional 3 hrs. Cells were then lysed in plate with 250 μl actin stabilization buffer (0.1 M PIPES, pH6.9, 30% glycerol, 5% DMSO, 1 mM $MgSO_4$, 2 μg/ml of each of leupeptin, pepstatin A and chymostatin) and incubated at 4°C for 20 min. Lysed cells were scraped out of the plate and ultracentrifuged (100,000 *g*) for 15 min at 4°C in Beckman TLA100.1 ultracentrifuge rotor (Beckman Coulter, Fullerton, CA). The supernatant was collected and used as the G-actin fraction. The pellet was dissolved in 250 μl lysis buffer supplemented with 5 μM cytochalasin D (Sigma), and used as the F-actin fraction. Equal percentages of the G-actin and F-actin fractions were resolved by SDS-PAGE and immunoblotted with antibodies that recognize actin, cortactin or α-actinin.

Proteomic analysis of polypeptides in the Alix complexes. Equally mixed 5 μg of 1A12, 1F7, 2H12 and 3A9 antibodies that were immobilized onto 40 μl protein G sepharose were incubated with 2 ml of WI38 cell lysates containing ~2 mg total proteins at 4°C overnight and washed six times with RIPA buffer. The immunocomplexes were then eluted with 80 μl of SDS-PAGE sample buffer and resolved by 10% SDS-PAGE. After the gels were silver stained, all visualized polypeptides that had been specifically precipitated by anti-Alix antibodies were excised and digested at 37°C overnight with 100 ng of modified trypsin (Promega, Madison, WI). After extraction and vacuum concentration, samples were analyzed with LC-MS/MS on an electrospray ion trap mass spectrometer (LCQ DecaXP, Thermo, San Jose, CA). The following aqueous solvent system was used: Solvent A contained 2% acetonitrile with 0.01% TFA, and Solvent B consisted of 20% 2-propanol, 60% acetonitrile, and 0.01% trifluoroacetic acid (TFA). The solvents were purchased from Burdick and Jackson (Muskegon, MI) and TFA was acquired from Pierce (Rockford, IL). The gradient was ramped from 5% B to 60% B over 40 minutes using an Ultimate pump (Dionex, Sunnyvale, CA). Tandem mass spectra were subjected to database searches using Mascot (http://www.matrixscience.com) for trypsin and semitrypsin enzyme specificities and allowing for methionine oxidation and as many as 2 missed cleavages.

RESULTS

Alix is required for WI38 cells to maintain typical fibroblast morphology. Our previous investigation of Alix's function in immortalized mouse fibroblast NIH/3T3 cells revealed roles of Alix in regulating fibroblast morphology. To determine whether this applies to the model system chosen for this study, we transfected WI38 cells with siRNA against either Alix or GFP (used as a negative control) and examined the effect of Alix knockdown on WI38 cell morphology. Immunoblotting of crude cell lysates with anti-Alix monoclonal antibodies generated by us showed that Alix expression decreased by 3-4 folds in Alix siRNA-transfected cells at 24 hrs and became hardly detectable at 48 - 96 hrs after the transfection, whereas actin expression did not decrease. In contrast to Alix siRNA-transfected cells, control transfected cells expressed constant levels of both Alix and actin (Fig. 1A). Parallel observation of the morphology of the transfected cells without a subculture revealed that Alix knockdown cells formed fewer membrane protrusions and looked blunter than control cells although overall cell

shapes were similar (Fig. 1B, upper panel). When control and Alix siRNA-transfected cells were first subcultured and then examined, the effect of Alix knockdown on cell morphology became more dramatic (Fig. 1B, lower panel) despite their comparable rates of cell growth and death (data not shown). These results indicated that Alix is required for WI38 cells to maintain typical fibroblast morphology.

Alix associates with actin cytoskeleton in WI38 cells. To investigate the role of Alix in the transmembrane network that regulates fibroblast morphology, we first determined the subcellular localization of Alix in WI38 cells in relation to F-actin based structures with 1A12, 1F7 and 3A9 anti-Alix monoclonal antibodies and the F-actin specific agent phalloidin (19, 20). These three antibodies were chosen because each efficiently immunoblotted and immunoprecipitated Alix in crude lysates of WI38 cells. We observed that each of the three antibodies stained F-actin based structures as well as free standing particles, which were probably endosomes based on previously established functions of Alix in endosomal sorting. In contrast, none of the antibodies stained structures at the cell periphery that assumed the shape of focal adhesions. As representatives, 3A9 antibody stained both protruding lamella at the cell edge and circumvential actin bundles at the base of the lamella in newly seeded cells that were spreading (Fig. 2A). In well spread cells, 3A9 antibody stained lamellipodia and stress fibers (Fig. 2B). When we cultured WI38 cells on fibronectin-coated substrata, which greatly enhanced stress fiber assembly, Alix almost quantitatively localized at stress fibers (Fig. 2C). These results demonstrated that Alix associates with actin cytoskeleton in WI38 cells.

Alix knockdown inhibits actin cytoskeleton assembly in WI38 cells . To determine whether Alix has functions in actin cytoskeleton assembly, we transfected WI38 cells with control or Alix specific siRNA and stained cells with phalloidin, which stains both F-actin that has been assembled into high order structures and short F-actin scattered in the cytoplasm (21-24). Clearly, the F-actin staining was universally weaker in Alix knockdown cells than in control cells. The difference was best illustrated by concurrent staining of the majority of Alix siRNA-transfected cells and the few non-transfected cells in the same field (Fig. 3A). However, no change was observed in the protein level of actin (Fig. 1A). Treatment of WI38 cells with the F-actin depolymerization agent cytochalasin D reduced the overall staining by phalloidin as well

(Fig. 3B). These results indicated that Alix knockdown inhibits F-actin formation in WI38 cells. In support of this conclusion, when crude lysates of control and Alix knockdown WI38 cells were fractionated into F-actin-containing and G-actin-containing fractions, the F-actin: G-actin ratio in control cell was ~ 3 fold higher than that in Alix knockdown cells (Fig. 3C).

In addition to the negative effect of Alix knockdown on the F-actin content, Alix knockdown cells also assembled less stress fibers than control cells, especially in central areas of the cell. This difference was most obvious when cells were grown on fibronectin-coated substrata, which enhances stress fiber assembly (Fig. 3D, left panel). In contrast, control and Alix knockdown cells formed comparable numbers of focal adhesions, as revealed by immunofluorescence staining of vinculin (Fig. 3D, middle panel), eliminating the possibility that Alix knockdown inhibits stress fiber assembly in WI38 cells through inhibiting integrin-mediated cell adhesions.

Alix directly interacts with actin. To characterize the mechanism by which Alix associates with actin cytoskeleton and promotes its assembly, we initially determined whether Alix directly interacts with actin. For this, we first induced polymerization of commercial G-actin in the presence of bacterially produced GST-Alix or GST alone and determine their interaction with F-actin by the F-actin co-sedimentation assay (25). As shown in Fig. 4, 30-70% of the four major polypeptides in the GST-Alix sample co-pelletted with F-actin whereas the negative control GST remained in the supernatant. Mass spec analyses of these four polypeptides revealed that they contained residues 1-802, 1-759, 1-745 and 1-574 of Alix, respectively (Fig. S2). These results indicated that an N-terminal region of Alix directly interacts with F-actin. To further characterize the region in Alix that interacts with F-actin, we produced GST-tagged Alix truncation products that lacked the N-terminal Bro1 domain (GST-AlixΔN), the C-terminal Pro-rich domain (GST-AlixΔC) or both of them (GST-AlixM) in bacteria and examined their interaction with F-actin by the F-actin cosedimentation assay. While GST-AlixΔN and GST-AlixΔC bound F-actin as efficiently as GST-Alix, GST-AlixM hardly bound F-actin (Fig. 4B). These results indicated that the N-terminal Bro1 domain and the C-terminal PRD of Alix may each contain a docking site for F-actin. To test this possibility, we next produced non-cleaved GST-Alix, GST-AlixΔN, GST-Bro1 and myc-tagged PRD plus the adjacent 100 residues of Alix

(myc-PRD+) by in vitro translation and determined their interaction with F-actin by the cosedimentation assay. PRD+ was myc tagged because it had already been produced for a separate study. Approximately 30~70% of GST-Alix, GST-AlixΔN, GST-Bro1 or myc-PRD+ cosedimented with F-actin (Fig. 4C), confirming that both the Bro1 domain and the PRD interact with F-actin. Finally, to determine whether Alix interacts with G-actin as well, we incubated various GST-tagged Alix products from bacteria with commercial G-actin and examined G-actin retention by the GST pulldown assay. A small percentage of G-actin input (5-10%) was pulled down by GST-Alix but not GST alone (Fig. 4D). While GST-Bro1, GST-AlixΔN, GST-AlixΔC pulled down similar amounts of G-actin as did GST-Alix, GST-AlixM pulled down little G-actin (Fig. 4E). These results indicated that the Bro1 domain and the PRD of Alix interact with G-actin as well although probably at a much lower affinity than with F-actin.

Alix interacts with F-actin in a dose-dependent and stoichiometric manner. To obtain insights into the mode of Alix/F-actin interaction, we performed two series of F-actin polymerization reactions in the presence of bacterially produced GST-AlixΔC followed by ultracentrifugation. GST-AlixΔC was used in this experiment because it contained less cleavage products than GST-Alix and could be quantitated more accurately. The first series consisted of a fixed concentration of G-actin (1.2 μM) and variable concentrations of GST-AlixΔC (0.06 – 1.0 μM). Since we had determined that ~30% of GST-AlixΔC was available for F-actin binding (data not shown), actin was in excess at all GST-AlixΔC concentrations. As shown in Fig. 5A, the amount of GST-AlixΔC that bound to F-actin increased in parallel with the amount of the input GST-AlixΔC, indicating that Alix binds to F-actin in a dose-dependent manner. The second series of reactions consisted of variable concentrations of G-actin (0 – 8 μM) and a fixed concentration of GST-AlixΔC (1 μM). As shown in Fig. 5B, the amount of GST-AlixΔC that bound to F-actin reached a plateau at 1.2 μM actin, implying that actin was in excess at and above this actin concentration whereas GST-AlixΔC was in excess below this actin concentration. Most importantly, at 0.6 μM actin, ~0.17 μM GST-AlixΔC co-pelletted with ~0.4 μM F-actin, indicating that on the average one molecule of GST-AlixΔC may bind two molecules of actin.

Alix is an abundant protein. Since actin is an abundant protein, the dose-dependent and stoichiometric interaction of Alix with F-actin in cell free systems raised the possibility that Alix is an abundant protein as well. To test this possibility, we immunoblotted 30 μg of total proteins from WI38 cells either together or in parallel with 200 ng of GST-tagged middle region of Alix (GST-AlixM) with 1F7 antibody and estimated the amount of Alix in the total cellular proteins. GST-AlixM was used as a standard because it was clearly separated from endogenous Alix by SDS-PAGE. 1F7 antibody was chosen because this antibody recognized GST-Alix and GST-AlixM at similar efficiencies (data not shown). To obtain a reference for quantifying immunoblot signals, serially diluted WI38 cell lysates were immunoblotted (Fig. 5C, upper panel). It was observed that 200 ng of GST-AlixM generated 3-fold higher signals than the Alix in the cellular proteins (Fig. 5C, lower panel). Taking the mass difference between GST-AlixM and Alix into consideration, we estimated that Alix accounts for 0.25% of the total proteins in WI38 cell lysates, placing Alix into the category of abundant F-actin proteins.

Actin is a major partner protein of Alix. Alix has been reported to associate with a variety of partner proteins that regulate apoptosis, endosomal sorting and endocytosis. To estimate the relative abundance of Alix in WI38 cell lysates that associates with F-actin, we induced actin polymerization in WI38 cell lysates for 30 min, centrifuged the end products to pellet polymerized actin and then determined the percentage of Alix that cosedimented with F-actin. By immunoblotting, ~50% of Alix in WI38 cell lysates co-pelletted with polymerized actin (Fig. 5D), whereas little Cdk4 (used as a negative control) was recovered in the pellet fraction (data not shown). These results indicated that actin is a major partner protein of Alix in WI38 cells. To further examine this issue, we immunoprecipitated crude lysates of WI38 cells grown under regular culture conditions with a combination of multiple anti-Alix monoclonal antibodies and analyzed the immunocomplexes by silver staining and mass spectrometry. As shown in Figure 5E, actin was the major non-IgG polypeptide detected in the Alix immunoprecipitate besides the full-length and cleaved Alix. In contrast, none of the previously identified Alix binding partners that should not be masked by the heavy and light chains of the precipitating antibodies were detected, indicative of their absence or low abundance in the Alix immunoprecipitate. Although the control precipitate contained actin as well, the level was much lower than in the Alix

immunoprecipitate and its presence could be eliminated by more thorough washing, which did not eliminate actin in the Alix immunoprecipitate (data not shown). The control immunoprecipitate also contained a protein that comigrated with Alix. However, mass spec analysis of this protein disproved its being Alix. These results further indicated that actin is a major partner protein of Alix in WI38 cells.

Alix interacts with cortactin. Since Alix is an adaptor protein, its interaction with F-actin and localization at lamellipodia raised the possibility that Alix interacts with an F-actin binding protein at lamellipodia. Cortactin is one of the major F-actin-binding proteins at lamellipodia where promotes and stabilizes ARP2/3 complex-induced actin network formation (26, 27). Since Cabezas et al showed in a recent study that Alix knockdown in HeLa cells caused abnormal distribution of endosomes and the cortical actin cytoskeleton proteins such as cortactin and clathrin (28), we explored the possibility that Alix interacts with cortactin. For this objective, we first double stained WI38 cells with anti-cortactin and anti-Alix antibodies. As shown in Fig. 6A, Alix staining colocalized with cortactin staining at lamellipodia. Second, we determined biochemical interaction of Alix with cortactin by coimmunoprecipitation and recombinant protein pulldown assays. After immunoprecipiation of WI38 cell lysates with anti-Alix antibodies or mouse IgG, cortactin was detected in the Alix immunoprecipitate but not in the control immunoprecipitate. Incubation of WI38 cell lysates with various Alix products followed by immunoblotting of the bound proteins with anti-cortactin antibodies showed that cortactin interacted with all of the Alix fragments that contained residues 436-609 (MB1) in the C-terminal half of the middle region (Fig. 6C), indicating that this non-actin binding region contains a cortactin docking site. Third, we determined the effects of Alix knockdown and cytochalasin D treatment on cortactin localization by immunofluorescence microscopy. Both Alix knockdown and cytochalasin D treatment reduced phalloidin staining and inhibited stress fiber assembly as described earlier. However, while cytochalasin D treatment did not eliminate cortactin localization at the cell periphery (Fig. S4) Alix knockdown cells completely abolished it (Fig. 6D). This was in contrast to no change in the level of cortactin expression in Alix knockdown cells (Fig. 6E). Finally, we determined the effect of Alix knockdown on the relative abundance of cortactin in the G-actin and F-actin fractions by biochemical approaches Alix

knockdown reduced the percentage of cortaictn in the F-actin fraction by two fold (Fig. 6F). Together, these results indicated that Alix directly interacts with cortactin and that this interaction plays important roles in localizing cortactin to lamellipodia.

Alix interacts with α-actinin. Alix association with stress fibers raised the possibility that Alix may interact with an F-actin binding protein that preferentially localizes at stress fibers. To explore this possibility, we investigated Alix interaction with α-actinin, an F-actin-bundling protein that primarily associates with stress fibers (29). By immunoprecipitation of WI38 cell lysates with anti-Alix or anti-α-actinin antibodies followed by reciprocal immunoblotting, Alix and α-actinin interacted with each other in WI38 cell lysates (Fig. 7A). Mapping the α-actinin binding region in Alix as we did for cortactin showed that it locates in the N-terminal portion of the middle region of Alix (residues 167-436, MA) (Fig. 7B), which bound neither F-actin (Fig. 4B) nor cortactin (Fig. 6B). Interestingly, the MA fragment consistently pulled down more α-actinin than the M fragment, suggesting that the MB fragment contains inhibitory sequences for Alix association with α-actinin. Next, we determined the effect of Alix knockdown on α-actinin association with F-actin and stress fibers. Although Alix knockdown did not affect α-actinin expression (Fig. 7C), Alix knockdown reduced the relative abundance of α-actinin in the F-actin fraction by two fold, as determined by immunoblotting of α-actinin in the G-actin and F-actin fractions in crude lysates of control and Alix-siRNA transfected cells (Fig. 7D). Moreover, when control and Alix knockdown cells grown on fibronectin-coated substrata were stained with anti-α-actinin antibodies, α-actinin assumed a pattern of stress fibers in control cells whereas it existed as clumps or thick bundles at the cell periphery in Alix knockdown cells (Fig. 7E). Together, these results indicated that Alix interacts with α-actinin and suggested that this interaction promotes α-actinin interaction with F-actin and its roles in stress fiber assembly.

Example 2

Cell culture and indirect immunofluorescence. WI38 cells were cultured in Eagle's Minimal Essential medium with Earle's Salts (Invitrogen, Carlsbad, CA) that was supplemented with 2 mM L-glutamine and 10% fetal bovine serum. Transfection of WI38 cells with GFP or Alix-specific siRNAs was performed as we described elsewhere (62). For indirect

immunofluorescence, WI38 cells were seeded on 22-mm glass coverslips placed in 35 mm dishes. In some experiments, the glass coverslips were pre-coated with 20 μg/ml purified human plasma fibronectin (Sigma, St. Louis, MO) at 4°C for overnight and blocked with 1% BSA at room temperature for 30 min. After the coated coverslips were washed three times with PBS, $1x10^4$ WI38 cells were seeded into each dish in regular culture medium. WI38 cells grown on the coated coverslips for indicated times were fixed with 4% paraformaldehyde, permeabilized with 0.5% Triton X-100, and blocked for 1 hr with 10% horse serum (Invitrogen) in phosphate-buffered saline (PBS). Fixed cells were first incubated for 2 hr with 1 μg/ml of primary antibodies diluted in 5% horse serum in PBS, followed by 3 rinses with PBS/0.1% NP-40 (Sigma), and then incubated for 1 hr with FITC-conjugated secondary antibody (Sigma) that was diluted 1:200 in 3% horse serum in PBS/0.1% NP-40. After 3 times rinses with PBS/0.1% NP-40, samples were counterstained with 2 μg/ml propidium iodide (Sigma) in PBS for 10 min. After 3 times of final wash, the stained cells were mounted with anti-fade (Vector laboratories, Burlingame, CA) and images were captured by the ZEISS Axioplan 2 imaging system (Carl Zeiss Microimaging Inc., Thornwood, NY).

Immuno-gold electron microscopy. WI38 cells grown on glass coverslips were fixed in situ for 1 h with 2% formalin (Ted Pella, Redding, CA) and 3% glutaraldehyde (Ted Pella) in 0.1 M sodium cacodylate (pH 7.3). After fixation, cells on coverslips were washed twice for 15 min each time with 0.05% Tween-20 in PBS (PBST), blocked for 1 h with 1% casein (BioRad, Philadelphia, PA) in PBS (blocking solution), and then incubated at 4°C overnight with 0.1 μg/ml 3A9 antibody in blocking solution. Subsequently, cells were washed three times for 15 min each time with PBST, incubated overnight with a 1:50 dilution of 1-nm gold-conjugated goat anti-mouse IgG (Ted Pella) in blocking solution, and washed again three times for 15 min each time with PBST. Cells were then re-fixed for 20 min with 2% glutaraldehyde in PBST, washed three times for 15 min each time with molecular-grade water, and silver enhanced with Light Insensitive Silver Enhancer (Ted Pella) for ~20 min. After enhancement, cells were washed three times for 10 min each time with molecular grade water and post-fixed again with 2% formalin and 3% glutaraldehyde in 0.1 M sodium cacodylate (pH 7.3). The post-fixed cells were embedded in spurr resin (Polysciences, Inc., Warrington, PA) on coverslips, sectioned after

the spur blocks were detached from coverslips, and analyzed by transmission electron microscopy as previously described (65).

Antibody labeling of live cells. Labeling of live WI38 cells with antibodies was performed on cells that had been grown on 22-mm glass coverslips for at least 24 hrs or cells that were kept in suspension after trypsinization. After cells were washed twice with ice-cold PBS and incubated in the cold PBS for 15 min, the labeling antibody was added at 1 μg/ml and cells were further incubated on ice for 30 min. Production and purification of antibodies are described are known (62). Neutralization of 1A12 antibody was achieved by incubation with 20 μg/ml GST-Alix. The antibody-labeled cells were washed, fixed in 4% paraformaldehyde, permeabilized with 0.5% Triton X-100 and blocked with 10% horse serum/PBS/0.1% NP-40. The cultures were then stained with FITC-conjugated secondary antibodies (Sigma) that were 1:200 diluted in 5% horse serum/1x PBS/0.1% NP-40 for 1 hr and then counterstained with TRITC-conjugated phalloidin (Sigma) for 40 min. The stained cells were mounted with anti-fade (Vector laboratories), and images were captured by the ZEISS Axioplan 2 imaging system (Carl Zeiss Microimaging Inc.).

Cell surface biotinylation, immunoprecipitation and immunoblotting. Sub-confluent WI38 cells grown in 100-mm culture dishes or trypsinzed WI38 cells in suspension were rinsed twice with ice-cold PBS, and exposed proteins were biotinylated by incubating cells with 2 ml of 0.5 mg/ml Sulfo-NHS-LC-Biotin (Pierce, Rockford, IL) at 4°C for 30 min. After the reaction was stopped by incubation of the cultures in TBS for 15 min, total proteins were extracted in lysis buffer (0.5% Triton X-100, 5mM EDTA, and 150 mM NaCl in 20 mM Tris-HCl, pH7.4). Collected cell lysates were centrifuged at 10,000 g for 30 min, and protein concentrations of supernatants were determined by using a DC protein assay kit purchased from Bio-Rad Laboratories (Hercules, CA). The cleared WI38 cell lysates containing ~ 50 μg total protein were incubated with 1 μg primary antibodies at 4°C for overnight, and followed by incubation with protein G sepharose beads (Amersham Biosciences, Piscataway, NJ) at 4°C for 1 hr. The beads were washed five times with the lysis buffer and the immunocomplexes bound to the beads were eluted by SDS-PAGE sample buffer and blotted with anti-Alix antibodies as previously described (80) or with streptavidin. Monoclonal antibody used for immunoprecipitating $\alpha_v\beta_3$

integrin (clone LM609) and polyclonal antibodies for immunoprecipitating $\alpha_5\beta_1$ integrin were purchased from Chemicon International, Inc. (Temecula, C).

Detection of Alix on the culture substratum. Non-tryptic detachment of WI38 cells from culture surfaces was achieved by incubating PBS-rinsed cultures in 100-mm dishes with 5 ml TNE buffer (10 mM Tris-HCl, 150 mM NaCl, 5 mM EDTA) plus 5 mM EGTA at 37°C for 30-60 min with occasional tapping until cells were completely detached. After the detached cells were collected and the materials left on the dish were rinsed with PBS, they were extracted with equal volumes of SDS-sample buffer for SDS-PAGE and immunoblotting.

Detection of Alix in the conditioned medium. To collect conditioned media from WI38 cell cultures, sub-confluent cultures grown in 100-mm culture dishes were switched to fresh culture medium supplemented with 0.01% fetal bovine serum and cultured further for 2 days. The conditioned medium was then collected and fractionated by consecutive centrifugation at 1000 *g* for 10 min, at 10,000 *g* for 30 min and at 100,000 *g* for 1 hr. The pelleted proteins were dissolved in SDS-PAGE sample buffer. The remaining supernatant from the last centrifugation were precipitated by 10% trichloroacetic acid (TCA) on ice for 1 hr and pelleted by centrifugation at 10,000 *g* for 15 min. The pellet was then washed twice with –20°C acetone, and the proteins in the pellet were dissolved in 8 M urea for immunoblot analysis. For gel filtration, the 100,000 g pellet fraction of the conditioned medium was re-suspended in RIPA buffer (1% NP-40, 0.5% DOC, 0.1% SDS and 150 mM NaCl in 20 mM Tris-HCl, pH7.4), and fractionated through a 40 ml Superose 6 (Amersham Biosciences, Piscataway, NJ) column pre-equilibrated in TBS (150 mM NaCl in 20 mM Tris-HCl, pH7.4). Proteins in collected 1-ml fractions were precipitated by TCA and washed as described and immunoblotted with anti-Alix antibodies.

Antibody blocking of cell attachment and spreading. WI38 cells were trypsinized and resuspended at $1x10^6$ cells/ml in serum-free medium containing 40 μg/ml mouse IgG or anti-Alix antibody and incubated at 4°C for 30 min. To blocking integrin functions, cells were incubated with anti-$\alpha_5\beta_1$ integrin serum at 1:1000 dilution or 2.5 μg/ml anti-$\alpha_v\beta_3$ integrin antibody. The cells were then plated in 48-well plates at $1x10^4$ cells/well and incubated at 37°C for 1 hr. After washing with PBS for three times, the cells attached to the substratum were stained with 0.5% crystal violet/70% ethanol for 20 min and washed three times with double

distilled H_2O. The stained cells on the dish were then observed under a light microscope. An arbitrary cross line in a fixed position was drawn in each well and the cells distributed on this line were counted. Cells from triplet wells were counted for each treatment.

RESULTS

Presence of Alix in the substratum and on the cell surface. We had previously observed that the anti-Alix monoclonal antibodies 1A12 and 3A9 not only stained the cytoplasm of WI38 cells but also generated above-background staining in the culture substrata, especially at high cell densities. Thus, to explore the extracellular allocation of Alix, we first investigated whether staining of the substratum by these anti-Alix antibodies was indeed due to Alix. For this, we transfected WI38 cells with GFP or Alix-specific siRNA, subcultured the cells onto coverslips and then performed immunofluorescence staining of control and Alix knockdown cells with 1A12 and 3A9 antibodies under identical conditions. Immunoblots of crude cell lysates demonstrated that Alix-specific siRNA dramatically and specifically reduced the Alix expression in WI38 cells as we previously observed (Figure 15A). Fluorescence images of the stained cells taken at identical exposure times showed that Alix knockdown cells had much reduced staining by 1A12 and 3A9 antibodies both in the cytoplasm and in the substratum (Figure 15B and data not shown). These results indicated that Alix is present in extracellular compartments in addition to its predominant intracellular distribution.

To further characterize Alix distribution in extracellular compartments, we performed immuno-gold labeling of WI38 cell cultures with 3A9 antibody and sectioned embedded samples for electron microscopy (EM). To our surprise, 3A9 antibody stained the substratum and the cell periphery but not the cytoplasm for the majority of cells examined. In the cell sagittal-sections, 3A9 antibody stained particles or clusters of particles that were present in all exposed areas of the substratum and certain areas of the apical cell surface and the cell-matrix interface (Figure 9A). Electron micrographs of the cell cross-sections showed that 3A9 antibody stained particles or clusters of particles that localized both on the cell surface and in the area beneath the plasma membrane (Figure 9B). In some of the cells, the cell periphery staining was enriched in the pole area of membrane protrusions (Figure 9C). The preferential staining of the substratum and the cell periphery was not observed with negative control antibodies including mouse IgG (data not

shown). These results indicated that extracellular Alix distributes both in the substratum and on the cell surface.

The preferential staining of Alix in the substratum and the cell periphery by 3A9 antibody in immuno-gold EM made us speculate that the cell fixation procedure for EM selectively changes the conformation of the cytoplasmic Alix and thus prevents it from being recognized by 3A9 antibody. To test this speculation, we fixed WI38 cell cultures with the fixative routinely used for EM (2% formalin and 3% glutaraldehyde in 0.1 M sodium cacodylate) and then stained the cells with 3A9 antibody by indirect immunofluorescence. By this hybrid procedure, 3A9 antibody did not generated positive staining in the cytoplasm above the level generated by mouse IgG, whereas it stained the substratum as well as particles/clumps presumably at the cell periphery (Figure 9D). Similar results were obtained when 1A12 antibody was examined likewise (data not shown). These results supported our speculation and indicated that the conformation of Alix in the substratum and at the cell periphery differs from that present in the cytoplasm.

Detection of exposed and full-length Alix in the substratum. To determine whether Alix in the substratum exists in an exposed form, we stained live cultures of WI38 cells with 1A12 and 3A9 antibodies or mouse IgG as a negative control. Both 1A12 and 3A9 antibodies stained fine particles that distributed across the substratum, whereas mouse IgG did not generate such staining (Figure 10A). Pre-incubation of 1A12 antibody with recombinant Alix completely eliminated the staining. The substratum staining was not observed when the cells were stained with antibodies that recognize the EGF receptor or the sub-plasma membrane protein clathrin (data not shown). These results indicated that exposed Alix is present in the substratum and possibly on the cell surface.

To determine whether Alix in the substratum is a full-length protein, we labeled exposed proteins in live cultures of WI38 cells with a non-membrane permeable biotinylation agent and immunoprecipitated both labeled and non-labeled Alix in crude cell lysates. We then resolved the immunocomplexes by SDS-PAGE and blotted polypeptides with anti-Alix antibodies (for total Alix) and streptavidin (for biotinylated Alix). In crude lysates of both control-treated and biotinylated cultures, anti-Alix antibodies readily detected the full-length Alix (Figure 10B, left

panel). In the Alix immunoprecipitates, anti-Alix antibodies readily detected not only the full-length Alix, but also a polypeptide of ~70 kDa in addition to heavy and light chains of IgG (Figure 10B, middle panel). Since the 70-kDa polypeptide was specifically immunoprecipitated by anti-Alix antibodies, this polypeptide was likely to be a cleaved product of Alix generated during the immunoprecipitation. In contrast to anti-Alix antibodies, streptavidin detected a single prominent polypeptide of ~95 kDa in the Alix immunoprecipitates from labeled cultures, which was absent in the Alix immunoprecipitates from mock-treated cultures or the mouse IgG precipitates from labeled cultures (Figure 10B, right panel). This polypeptide co-migrated with the full-length Alix detected by anti-Alix antibodies in crude cell lysates or Alix immunoprecipitates. These results indicated that full-length Alix is present in the substratum. To further examine this issue, we detached WI38 cells from the substratum by EGTA, extracted proteins from both collected cells and the remaining extracellular matrix, and immunoblotted equivalent percentages of the cellular and matrix proteins by anti-Alix antibodies. As expected, the level of the cytoplasmic Alix greatly exceeded the level of the extracellular Alix. Most importantly, only full-length Alix was detectable in the extracellular fraction of the proteins, whereas both full-length and cleaved products of Alix were detectable in crude cell lysates (Figure 10C). Even after much extended exposure of the blots, cleaved products of Alix were still undetectable in the substratum proteins (data not shown). These results further demonstrated that full-length Alix is present in the substratum.

Detection of exposed and full-length Alix on the cell surface. Besides homogeneously staining of the substratum, 1A12 and 3A9 antibodies also stained particles that sparsely scattered on the cell surface (data not shown), consistent with much lower abundance of Alix on the cell surface than the substratum as revealed by immuno-gold EM (Figure 9). This suggested that exposed Alix is also present on the cell surface. To test this, we detached WI38 cells from culture substrata by brief trypsinization and stained live cells in suspension with 1A12 and 3A9 antibodies or the negative control antibody mouse IgG at 4°C. By this method, only exposed Alix on the cell surface could be bound by 1A12 and 3A9 antibodies although some of the immunocomplexes might be clustered and internalized during the incubation. As shown in Figure 11A, both 1A12 and 3A9 antibodies stained particles or clumps that were

heterogeneously distributed among the cells, whereas mouse IgG only generated low levels of diffused staining. These results indicated that exposed Alix is present at least in certain areas of the cell surface. To determine whether the exposed Alix on the cell surface is a full-length protein, we made crude lysates of washed cells and recovered the immunocomplexes by affinity absorption with protein G-sepharose. Immunoblotting of the polypeptides in the immunocomplexes by anti-Alix antibodies showed that 1A12 or 3A9 antibody bound full-length Alix whereas mouse IgG did not (Figure 11B). In addition, we biotinylated live WI38 cells in suspension and determined Alix biotinylation by blotting Alix immunoprecipitates with streptavidin. As shown in Figure 11C, the predominant polypeptide that streptavidin specifically detected in the Alix immunoprecipitates had the molecular weight of full-length Alix. Together, these results indicated that full-length Alix is present on the cell surface.

Detection of high molecular weight complexes of Alix in the conditioned medium. The universal distribution of Alix in the substratum of WI38 cell cultures predicted that it was originated from Alix secreted into the culture medium by WI38 cells. To test this, we determined whether the conditioned culture medium contained full-length Alix that could not be accounted for by cell lysis. For this objective, we fractionated the conditioned medium collected from near confluent WI38 cell cultures into four fractions by sequential centrifugation (45) and immunoblotted them with anti-Alix antibodies. As shown in Figure 12A, Alix was undetectable in the 1,000 g and 10,000 g pellets, which presumably contained dead cells and large membrane debris, respectively, indicating negligible levels of cell lysis. In contrast, full-length Alix was readily and reproducibly detected in the 100,000 g pellet, which presumably contained large protein complexes/small membrane vesicles. In the TCA precipitate of 100,000 g supernatant, which contained the remaining non-pelletable proteins, a truncated, but not full-length form of Alix, was detectable; however, its abundance was much lower than that in the 100,000 g pellet. This truncated Alix in the non-pelletable fraction probably resulted from low levels of cell lysis. These results indicated that full-length Alix, which existed either in huge protein complexes or within small membrane vesicles, is secreted into the conditioned medium. To distinguish between these two possibilities, we resuspended the 100,000 g pellet in membrane-dissolving RIPA buffer and fractionated the sample in parallel with crude lysates of WI38 cells by gel

filtration through Superose 6, which has an exclusion limit of 5000 kDa. Determination of the elution profile of Alix from the two different gel filtrations by immunoblotting showed that Alix from the medium sample was exclusively eluted in the void volume (Figure 12B, upper panel), supporting the possibility that Alix in the conditioned medium exists in large protein complexes. In contrast, the majority of Alix from crude cell lysates was eluted in the 158 kDa fractions, and only ~5% of Alix was eluted in the void volume (Figure 12B, bottom panel). The latter minor portion might represent the subpopulation of Alix at the cell periphery. These results indicated that Alix in the conditioned medium exists in much bigger protein complexes than the predominant cytoplasmic Alix.

Inhibition of integrin-mediated cell adhesions by antibody binding to extracellular Alix. To explore the potential role of extracellular Alix in cell adhesions, we first incubated WI38 cells in suspension with 1A12/3A9 antibody or mouse IgG (used as a negative control) and determined the effect of antibody binding to the extracellular Alix on the initial rate of cell attachment. Counts of cell numbers at 1 h after cell seeding showed that both 1A12 and 3A9 antibodies caused a great reduction (50%~70%) in the number of attached cells (Figure 13A). We then transfected WI38 cells with control or Alix siRNA and determined the effect of 1A12 antibody on attachment of control and Alix knockdown cells. Although 1A12 antibody caused 80% inhibition in control siRNA-transfected cells, the antibody caused less than 20% inhibition in Alix siRNA-transfected cells, which had much reduced expression of Alix (Figure 13B). These results indicated that antibody binding to the extracellular Alix has negative effects on cell attachment to the substratum.

Cell attachment to the substratum is determined by a variety of integrin-mediated cell adhesions (57). WI38 cells express the vitronectin receptors $\alpha_v\beta_3$ and α_v/β_1 integrins, fibronectin receptors α_5/β_1 and α_v/β_1 integrins and collagen receptors α_1/β_1, α_2/β_1, α_3/β_1 and α_6/β_1 (75). To determine whether antibody binding to extracellular Alix inhibits specific integrin-mediated cell adhesions, we coated culture surfaces with the ECM protein fibronectin, vitronectin or collagen or the negative control polypeptide poly-L-lysine and determined the effect of 1A12 antibody on cell attachment. While 1A12 antibody caused 55% and 70% inhibition in cell attachment to fibronectin- and vitronectin-coated substrata, respectively, this antibody did not affect cell

attachment to collagen- or poly-L-lysine-coated substrata (Figure 13C). 1A12 antibody also severely inhibited spreading of attached cells on vitronectin-coated substrata (Figure 13D) and moderately inhibited spreading of attached cells on fibronectin-coated substrata (data not shown). In our pilot experiments, functional blocking antibodies against α_5/β_1 and α_v/β_3 integrin appears to inhibits ~ 80% of WI38 cell attachment to fibronectin and vitronectin, respectively (data not shown), indicating that, in this cell line, α_5/β_1 and α_v/β_3 are the major cell surface receptors for fibronectin and vitronectin, respectively. Therefore, the inhibitory function of 1A12 on WI38 cell attachment and spreading on vitronectin and fibronectin indicated that antibody binding to the extracellular Alix inhibits α_v/β_3 integrin-mediated cell adhesion and possibly also α_5/β_1 integrin-mediated cell adhesions.

Physical linkage of Alix to αv/β3 integrin. The ability of anti-Alix antibodies to inhibit α_v/β_3 and possibly also α_5/β_1 integrin-mediated cell adhesions raised the possibility that extracellular Alix physically associates with these integrins. To test this possibility, we biotinylated surface proteins in cultures of control or Alix knockdown WI38 cells and immunoprecipitated crude lysates of the labeled cells with anti-α_v/β_3 or anti-α_5/β_1 antibodies. We then blotted the precipitated proteins with streptavidin and determined whether biotinylated Alix co-immunoprecipitated with either α_v/β_3 or α_5/β_1 integrin. As shown in Figure 14A, the α_v/β_3 integrin immunocomplex from control cells contained not only biotinylated α_v and β_3 integrins but also a polypeptide of ~95 kDa, whereas the α_v/β_3 integrin immunocomplex from Alix knockdown cells contained only biotinylated α_v and β_3 integrins. The Alix-dependent extra polypeptide migrated slightly slower than Alix in crude cell lysates (data not shown). In contrast, the α_5/β_1 integrin immunocomplex from both control and Alix knockdown cells contained only biotinylated α_5 and β_1 integrins and lacked the ~95 kDa polypeptide. These results indicated that Alix on the cell surface is physically linked to α_v/β_3 integrin. To further examine this possibility, we immunoprecipitated crude lysates of WI38 cells with anti-α_v/β_3 integrin antibodies, anti-α_5/β_1 integrin antibodies, or mouse IgG (used as a negative control) and immunoblotted different immunocomplexes with anti-Alix antibodies. While mouse IgG did not pulled down Alix as expected, the anti-α_v/β_3 antibodies pulled down a doublet of Alix, the upper band of which

migrated slower than the detected Alix in crude cell lysates (Figure 14B), suggesting a post-translational modification. We suspected that this upper band might represent the above-mentioned extra polypeptide in the α_v/β_3 integrin immunocomplex since the latter also migrated slower than the detected Alix in crude cell lysates. In contrast to anti-α_v/β_3 integrin antibodies, anti-α_5/β_1 antibodies did not pull down detectable amounts of Alix (data not shown). These results supported the possibility that Alix physically associates with α_v/β_3 integrin on the cell surface.

Enhancement of α_v/β_3 integrin-mediated cell adhesion by reducing the Alix expression. Since Alix on the cell surface physically associates with α_v/β_3 integrin, antibody binding to the cell surface Alix might produce physical hindrance to α_v/β_3 integrin, thus inhibiting its proper functions. This made it difficult to ascertain whether Alix on the cell surface is a positive or negative regulator of α_v/β_3 integrin-mediated cell adhesion. To address this issue, we transfected WI38 cells with control or Alix-specific siRNAs and determined the effect of Alix knockdown on α_v/β_3 and α_5/β_1 integrin-mediated cell adhesions. Initially, we incubated control and Alix knockdown cells with anti-α_v/β_3 or anti-antibodies and determined the percentage of inhibition of cell attachment in each case. As shown in Figure 14C, Alix knockdown increased the inhibition caused by anti-α_v/β_3 integrin antibodies from 46% to 75%, whereas it decreased the inhibition caused by anti-α_5/β_1 integrin antibodies from 85% to 65%. These results indicated that Alix is a negative regulator of α_v/β_3 integrin mediated cell adhesion. Further, we stained the newly attached control and Alix knockdown WI38 cells in parallel with antibodies that recognize α_v/β_3 or α_5/β_1 integrin. In principle, α_v/β_3 only forms focal adhesion at the cell periphery, whereas α_5/β_1 integrin forms both focal adhesions at the cell periphery and fibrillar adhesions in the central area of the cell. The fibrillar adhesions result from centripetal translocation of α_5/β_1 integrin from focal adhesion (63). Fluorescent images taken at identical exposure times showed that reducing Alix expression increased the size and abundance of α_v/β_3 integrin-mediated focal adhesion at the cell periphery. Meanwhile, it increased the size of α_5/β_1 integrin-mediated focal adhesions at the cell periphery, but eliminated α_5/β_1 integrin-mediated adhesions in the central

area of the cells (Figure 14D). These results indicated that Alix both inhibits α_v/β_3 integrin-mediated cell adhesion and promotes α_5/β_1 integrin-mediated fibrillar adhesion.

Therefore, the present invention is well adapted to attain the ends and advantages mentioned as well as those that are inherent therein. While numerous changes may be made by those skilled in the art, such changes are encompassed within the spirit of this invention as illustrated, in part, by the appended claims.

References

1. Mitchison, T. J., and Cramer, L. P. (1996) *Cell* 84(3), 371-379

2. Pollard, T. D., and Borisy, G. G. (2003) *Cell* 112(4), 453-465

3. Brakebusch, C., and Fassler, R. (2003) *Embo J* 22(10), 2324-2333

4. Blystone, S. D. (2004) *Biochim Biophys Acta* 1692(2-3), 47-54

5. Pawlak, G., and Helfman, D. M. (2001) *Curr Opin Genet Dev* 11(1), 41-47

6. Kahn, P., Heller, D., and Shin, S. (1983) *Cytogenet Cell Genet* 36(4), 605-611

7. Labat-Robert, J. (2002) *Semin Cancer Biol* 12(3), 187-195

8. Sadoul, R. (2006) *Biol Cell* 98(1), 69-77

9. Trioulier, Y., Torch, S., Blot, B., Cristina, N., Chatellard-Causse, C., Verna, J. M., and Sadoul, R. (2004) *J Biol Chem* 279(3), 2046-2052. Epub 2003 Oct 2029.

10. Luhtala, N., and Odorizzi, G. (2004) *J Cell Biol* 166(5), 717-729

11. Matsuo, H., Chevallier, J., Mayran, N., Le Blanc, I., Ferguson, C., Faure, J., Blanc, N. S., Matile, S., Dubochet, J., Sadoul, R., Parton, R. G., Vilbois, F., and Gruenberg, J. (2004) *Science* 303(5657), 531-534.

12. Kim, J., Sitaraman, S., Hierro, A., Beach, B. M., Odorizzi, G., and Hurley, J. H. (2005) *Dev Cell* 8(6), 937-947

13. Krebs, J., and Klemenz, R. (2000) *Biochim Biophys Acta* 1498(2-3), 153-161.

14. Shibata, H., Yamada, K., Mizuno, T., Yorikawa, C., Takahashi, H., Satoh, H., Kitaura, Y., and Maki, M. (2004) *J Biochem (Tokyo)* 135(1), 117-128

15. Elbashir, S. M., Harborth, J., Lendeckel, W., Yalcin, A., Weber, K., and Tuschl, T. (2001) *Nature* 411(6836), 494-498.

16. He, G., Siddik, Z. H., Huang, Z., Khokhar, A. R., and Kuang, J. (2005), *Oncogene*, 24 (18), 2929-43.

17. Yates-Siilata, K. E., Dahms, T. E., Webster, R. O., and Heuertz, R. M. (2004) *Cell Biol Int* 28(1), 33-39

18. Banan, A., Zhang, Y., Losurdo, J., and Keshavarzian, A. (2000) *Gut* 46(6), 830-837

19. Wulf, E., Deboben, A., Bautz, F. A., Faulstich, H., and Wieland, T. (1979) *Proc Natl Acad Sci U S A* 76(9), 4498-4502

20. Lengsfeld, A. M., Low, I., Wieland, T., Dancker, P., and Hasselbach, W. (1974) *Proc Natl Acad Sci U S A* 71(7), 2803-2807

21. Verderame, M., Alcorta, D., Egnor, M., Smith, K., and Pollack, R. (1980) *Proc Natl Acad Sci U S A* 77(11), 6624-6628

22. Carter, C. A., Doherty, M. M., Rusnak, D. W., Nettesheim, P., and Ferriola, P. C. (1994) *Exp Cell Res* 212(1), 141-150

23. Bereiter-Hahn, J., and Kajstura, J. (1988) *Histochemistry* 90(4), 271-276

24. Amankwah, K. S., and De Boni, U. (1994) *Exp Cell Res* 210(2), 315-325

25. Jongstra-Bilen, J., Janmey, P. A., Hartwig, J. H., Galea, S., and Jongstra, J. (1992) *J Cell Biol* 118(6), 1443-1453

26. Daly, R. J. (2004) *Biochem J* 382(Pt 1), 13-25

27. Kinley, A. W., Weed, S. A., Weaver, A. M., Karginov, A. V., Bissonette, E., Cooper, J. A., and Parsons, J. T. (2003) *Curr Biol* 13(5), 384-393

28. Cabezas, A., Bache, K. G., Brech, A., and Stenmark, H. (2005) *J Cell Sci* 118(Pt 12), 2625-2635

29. Otey, C. A., and Carpen, O. (2004) *Cell Motil Cytoskeleton* 58(2), 104-111

30. Weaver, A. M., Young, M. E., Lee, W. L., and Cooper, J. A. (2003) *Curr Opin Cell Biol* 15(1), 23-30

31. Pollard, T. D., and Beltzner, C. C. (2002) *Curr Opin Struct Biol* 12(6), 768-774

32. Higgs, H. N., and Pollard, T. D. (2001) *Annu Rev Biochem* 70, 649-676

33. Nickas, M. E., and Yaffe, M. P. (1996) *Mol Cell Biol* 16(6), 2585-2593.

34. Kubler, E., and Riezman, H. (1993) *Embo J* 12(7), 2855-2862

35. Nakamura, K., Fujita, A., Murata, T., Watanabe, G., Mori, C., Fujita, J., Watanabe, N., Ishizaki, T., Yoshida, O., and Narumiya, S. (1999) *FEBS Lett* 445, 9-13

36. Peck, J. W., Oberst, M., Bouker, K. B., Bowden, E., and Burbelo, P. D. (2002) *J Biol Chem* 277(46), 43924-43932

37. Akimov, S.S., Krylov, D., Fleischman, L.F., and Belkin, A.M. (2000). Tissue transglutaminase is an integrin-binding adhesion coreceptor for fibronectin. J Cell Biol *148*, 825-838.

38. Akiyama, S.K. (1996). Integrins in cell adhesion and signaling. Hum Cell *9*, 181-186.

39. Arroyo, R., and Orozco, E. (1987). Localization and identification of an Entamoeba histolytica adhesin. Mol Biochem Parasitol *23*, 151-158.

40. Banuelos, C., Garcia-Rivera, G., Lopez-Reyes, I., and Orozco, E. (2005). Functional characterization of EhADH112: an Entamoeba histolytica Bro1 domain-containing protein. Exp Parasitol *110*, 292-297.

41. Chatellard-Causse, C., Blot, B., Cristina, N., Torch, S., Missotten, M., and Sadoul, R. (2002). Alix (ALG-2-interacting protein X), a protein involved in apoptosis, binds to endophilins and induces cytoplasmic vacuolization. J Biol Chem *277*, 29108-29115. Epub 22002 May 29128.

42. Chen, B., Borinstein, S.C., Gillis, J., Sykes, V.W., and Bogler, O. (2000). The glioma-associated protein SETA interacts with AIP1/Alix and ALG-2 and modulates apoptosis in astrocytes. J Biol Chem *275*, 19275-19281.

43. Danen, E.H., Sonneveld, P., Brakebusch, C., Fassler, R., and Sonnenberg, A. (2002). The fibronectin-binding integrins alpha5beta1 and alphavbeta3 differentially modulate RhoA-GTP loading, organization of cell matrix adhesions, and fibronectin fibrillogenesis. J Cell Biol *159*, 1071-1086.

44. Dinter, A., and Berger, E.G. (1998). Golgi-disturbing agents. Histochem Cell Biol *109*, 571-590.

45. Fevrier, B., Vilette, D., Archer, F., Loew, D., Faigle, W., Vidal, M., Laude, H., and Raposo, G. (2004). Cells release prions in association with exosomes. Proc Natl Acad Sci U S A *101*, 9683-9688.

46. Garcia-Rivera, G., Arroyo, R., Mena, R., Luna, J., and Orozco, E. (1997). Involvement of the 112 kDa adhesin in Entamoeba histolytica phagocytosis. Arch Med Res *28 Spec No*, 166-167.

47. Garcia-Rivera, G., Rodriguez, M.A., Ocadiz, R., Martinez-Lopez, M.C., Arroyo, R., Gonzalez-Robles, A., and Orozco, E. (1999). Entamoeba histolytica : a novel cysteine protease and an adhesin form the 112 kDa surface protein. Mol Microbiol *33*, 556-568.

48. Geiger, B., Bershadsky, A., Pankov, R., and Yamada, K.M. (2001). Transmembrane crosstalk between the extracellular matrix--cytoskeleton crosstalk. Nat Rev Mol Cell Biol *2*, 793-805.

49. Ginsberg, M.H., Partridge, A., and Shattil, S.J. (2005). Integrin regulation. Curr Opin Cell Biol *17*, 509-516.

50. Hay, E.D. (1981). Extracellular matrix. J Cell Biol *91*, 205s-223s.

51. Katoh, K., Shibata, H., Hatta, K., and Maki, M. (2004). CHMP4b is a major binding partner of the ALG-2-interacting protein Alix among the three CHMP4 isoforms. Arch Biochem Biophys *421*, 159-165.

52. Katoh, K., Shibata, H., Suzuki, H., Nara, A., Ishidoh, K., Kominami, E., Yoshimori, T., and Maki, M. (2003). The ALG-2-interacting protein Alix associates with CHMP4b, a human homologue of yeast Snf7 that is involved in multivesicular body sorting. J Biol Chem *278*, 39104-39113. Epub 32003 Jul 39114.

53. Katzmann, D.J., Odorizzi, G., and Emr, S.D. (2002). Receptor downregulation and multivesicular-body sorting. Nat Rev Mol Cell Biol *3*, 893-905.

54. Kloc, M., Dougherty, M.T., Bilinski, S., Chan, A.P., Brey, E., King, M.L., Patrick, C.W., Jr., and Etkin, L.D. (2002). Three-dimensional ultrastructural analysis of RNA distribution within germinal granules of Xenopus. Dev Biol *241*, 79-93.

55. Martinez-Lopez, C., Orozco, E., Sanchez, T., Garcia-Perez, R.M., Hernandez-Hernandez, F., and Rodriguez, M.A. (2004). The EhADH112 recombinant polypeptide inhibits cell destruction and liver abscess formation by Entamoeba histolytica trophozoites. Cell Microbiol *6*, 367-376.

56. Mehul, B., and Hughes, R.C. (1997). Plasma membrane targetting, vesicular budding and release of galectin 3 from the cytoplasm of mammalian cells during secretion. J Cell Sci *110 (Pt 10)*, 1169-1178.

57. Miranti, C.K., and Brugge, J.S. (2002). Sensing the environment: a historical perspective on integrin signal transduction. Nat Cell Biol *4*, E83-90.

58. Missotten, M., Nichols, A., Rieger, K., and Sadoul, R. (1999). Alix, a novel mouse protein undergoing calcium-dependent interaction with the apoptosis-linked-gene 2 (ALG-2) protein. Cell Death Differ *6*, 124-129.

59. Murphy-Ullrich, J.E. (2001). The de-adhesive activity of matricellular proteins: is intermediate cell adhesion an adaptive state? J Clin Invest *107*, 785-790.

60. Nickel, W. (2003). The mystery of nonclassical protein secretion. A current view on cargo proteins and potential export routes. Eur J Biochem *270*, 2109-2119.

61. Odorizzi, G., Katzmann, D.J., Babst, M., Audhya, A., and Emr, S.D. (2003). Bro1 is an endosome-associated protein that functions in the MVB pathway in Saccharomyces cerevisiae. J Cell Sci *116*, 1893-1903. Epub 2003 Mar 1818.

62. Pan S, W.R., He G, Koomen J, Kobayashi R, Gallick GE, Sun L, Corvera J and Kuang J. A novel key function of Alix: direct regulation of the actin cytoskeleton. Journal of Biological Chemistry (manuscript in revision).

63. Pankov, R., Cukierman, E., Katz, B.Z., Matsumoto, K., Lin, D.C., Lin, S., Hahn, C., and Yamada, K.M. (2000). Integrin dynamics and matrix assembly: tensin-dependent translocation of alpha(5)beta(1) integrins promotes early fibronectin fibrillogenesis. J Cell Biol *148*, 1075-1090.

64. Peck, J.W., Bowden, E.T., and Burbelo, P.D. (2004). Structure and function of human Vps20 and Snf7 proteins. Biochem J *377*, 693-700.

65. Pelham, H.R. (1991). Multiple targets for brefeldin A. Cell *67*, 449-451.

66. Rodriguez, M.A., Hernandez, F., Santos, L., Valdez, A., and Orozco, E. (1989). Entamoeba histolytica: molecules involved in the target cell-parasite relationship. Mol Biochem Parasitol *37*, 87-99.

67. Ruoslahti, E. (1988). Fibronectin and its receptors. Annu Rev Biochem *57*, 375-413.

Sadoul, R. (2006). Do Alix and ALG-2 really control endosomes for better or for worse? Biol Cell *98*, 69-77.

68. Schmidt, M.H., Chen, B., Randazzo, L.M., and Bogler, O. (2003). SETA/CIN85/Ruk and its binding partner AIP1 associate with diverse cytoskeletal elements, including FAKs, and modulate cell adhesion. J Cell Sci *116*, 2845-2855. Epub 2003 May 2827.

69. Schmidt, M.H., Hoeller, D., Yu, J., Furnari, F.B., Cavenee, W.K., Dikic, I., and Bogler, O. (2004). Alix/AIP1 antagonizes epidermal growth factor receptor downregulation by the Cbl-SETA/CIN85 complex. Mol Cell Biol *24*, 8981-8993.

70. Stein, J.M., and Luzio, J.P. (1991). Ectocytosis caused by sublytic autologous complement attack on human neutrophils. The sorting of endogenous plasma-membrane proteins and lipids into shed vesicles. Biochem J *274 (Pt 2)*, 381-386.

71. Strack, B., Calistri, A., Craig, S., Popova, E., and Gottlinger, H.G. (2003). AIP1/ALIX is a binding partner for HIV-1 p6 and EIAV p9 functioning in virus budding. Cell *114*, 689-699.

72. Stupack, D.G., and Cheresh, D.A. (2002). Get a ligand, get a life: integrins, signaling and cell survival. J Cell Sci *115*, 3729-3738.

73. Thery, C., Boussac, M., Veron, P., Ricciardi-Castagnoli, P., Raposo, G., Garin, J., and Amigorena, S. (2001). Proteomic analysis of dendritic cell-derived exosomes: a secreted subcellular compartment distinct from apoptotic vesicles. J Immunol *166*, 7309-7318.

74. Vito, P., Pellegrini, L., Guiet, C., and D'Adamio, L. (1999). Cloning of AIP1, a novel protein that associates with the apoptosis-linked gene ALG-2 in a Ca2+-dependent reaction. J Biol Chem *274*, 1533-1540.

75. Vogel, B.E., Tarone, G., Giancotti, F.G., Gailit, J., and Ruoslahti, E. (1990). A novel fibronectin receptor with an unexpected subunit composition (alpha v beta 1). J Biol Chem *265*, 5934-5937.

76. von Schwedler, U.K., Stuchell, M., Muller, B., Ward, D.M., Chung, H.Y., Morita, E., Wang, H.E., Davis, T., He, G.P., Cimbora, D.M., Scott, A., Krausslich, H.G., Kaplan, J., Morham, S.G., and Sundquist, W.I. (2003). The protein network of HIV budding. Cell *114*, 701-713.

77. Wei, Y., Czekay, R.P., Robillard, L., Kugler, M.C., Zhang, F., Kim, K.K., Xiong, J.P., Humphries, M.J., and Chapman, H.A. (2005). Regulation of alpha5beta1 integrin conformation and function by urokinase receptor binding. J Cell Biol *168*, 501-511.

78. Wei, Y., Lukashev, M., Simon, D.I., Bodary, S.C., Rosenberg, S., Doyle, M.V., and Chapman, H.A. (1996). Regulation of integrin function by the urokinase receptor. Science *273*, 1551-1555.

79. Wu, Y., Pan, S., Che, S., He, G., Nelman-Gonzalez, M., Weil, M.M., and Kuang, J. (2001). Overexpression of Hp95 induces G1 phase arrest in confluent HeLa cells. Differentiation *67*, 139-153.

80. Wu, Y., Pan, S., Luo, W., Lin, S.H., and Kuang, J. (2002). Hp95 promotes anoikis and inhibits tumorigenicity of HeLa cells. Oncogene *21*, 6801-6808.

81. Xu, W., and Mitchell, A.P. (2001). Yeast PalA/AIP1/Alix homolog Rim20p associates with a PEST-like region and is required for its proteolytic cleavage. J Bacteriol *183*, 6917-6923.

82. Zhou X, P.S., Wang R, Sun L, Corvera J, Gallick G, Kuang J. (2006). The calcium modulated protein ALG-2 activates Alix's function in endosomal sorting (Submitted manuscript).

What is claimed is:

1. An antibody that binds to both denatured and non-denatured Alix, or epitope thereof.

2. An antibody as defined in claim 1, which is chimeric.

3. An antibody as defined in claim 1, which is humanly acceptable.

4. An antibody as defined in claim 1, which is conjugated to an anti-tumor agent.

5. An antibody as defined in claim 1, which is a monoclonal antibody.

6. A hybridoma clone of an antibody that binds to both denatured and non-denatured Alix, or epitope thereof.

7. An antibody that binds to extracellular Alix, or epitope thereof.

8. An antibody as defined in claim 7, which is chimeric.

9. An antibody as defined in claim 7, which is humanly acceptable.

10. An antibody as defined in claim 7, which is conjugated to an anti-tumor agent.

11. An antibody as defined in claim 7, which is a monoclonal antibody.

12. A hybridoma clone of an antibody that binds to extracellular Alix, or epitope thereof.

13. An antibody that binds to a region around amino acid residue 436 of Alix, or epitope thereof.

14. An antibody as defined in claim 13, which is chimeric.

15. An antibody as defined in claim 13, which is humanly acceptable.

16. An antibody as defined in claim 13, which is conjugated to an anti-tumor agent.

17. An antibody as defined in claim 13, which is a monoclonal antibody.

18. A hybridoma clone of an antibody that binds to a region around amino acid residue 436 of Alix, or epitope thereof.

19. A method of producing an antibody that binds to Alix comprising the steps of:

providing a tagged Alix protein;

introducing the tagged Alix protein into a subject;

removing a tissue sample from the subject; and

extracting from the tissue sample an antibody that binds to Alix.

20. The method of claim 19 wherein the tagged Alix protein comprises a fluorescent tag.

FIGURES

Figure 1

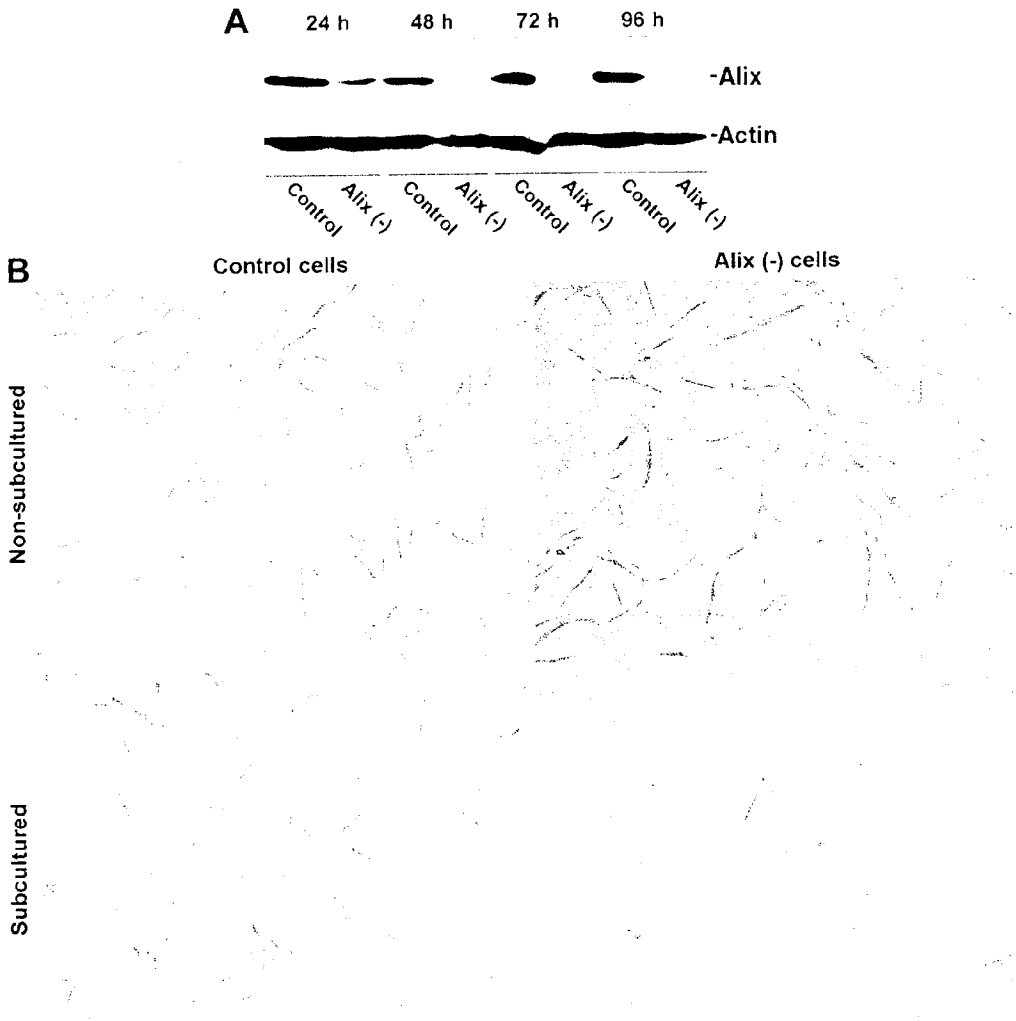

Figure 2

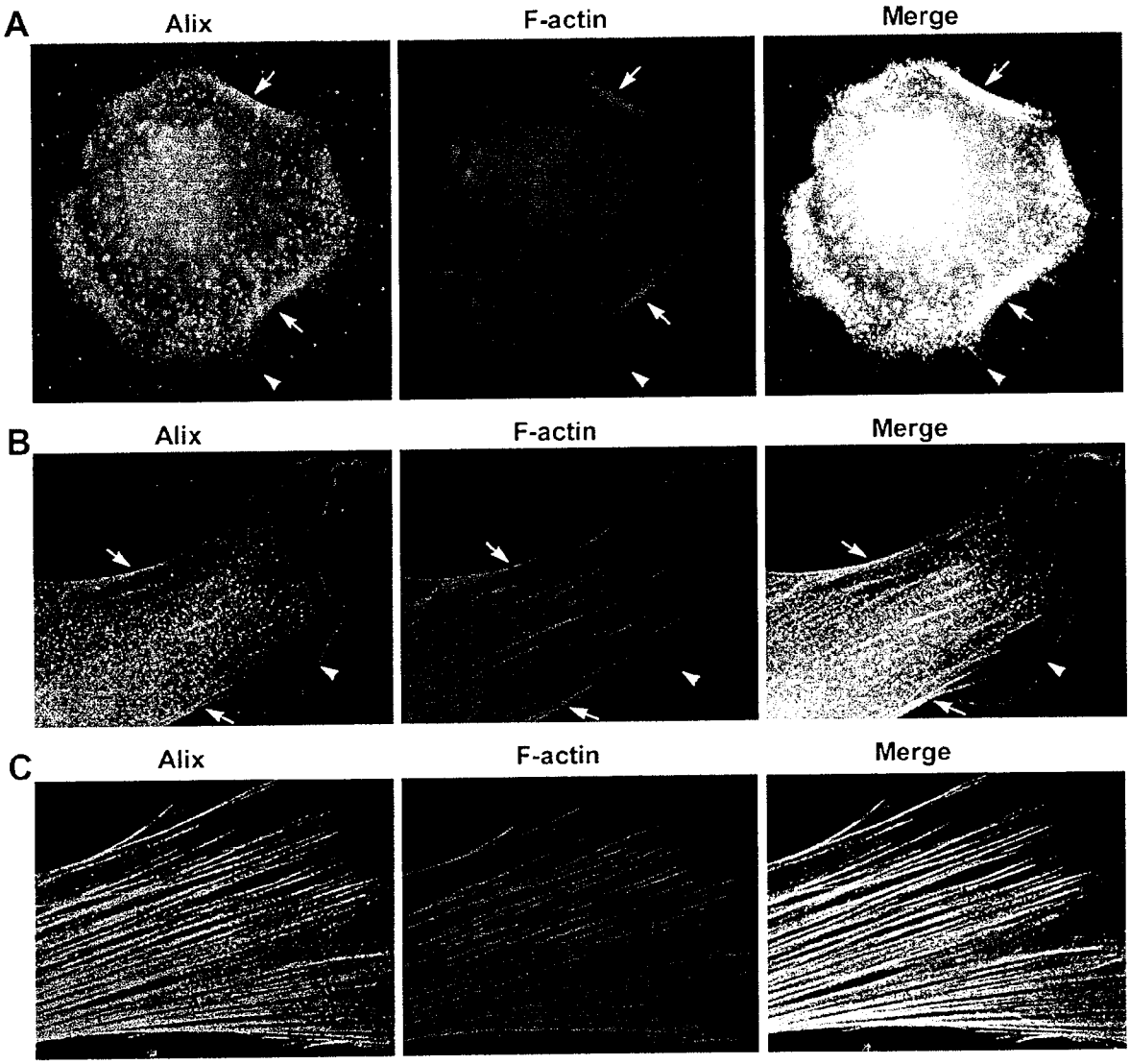

Figure 3

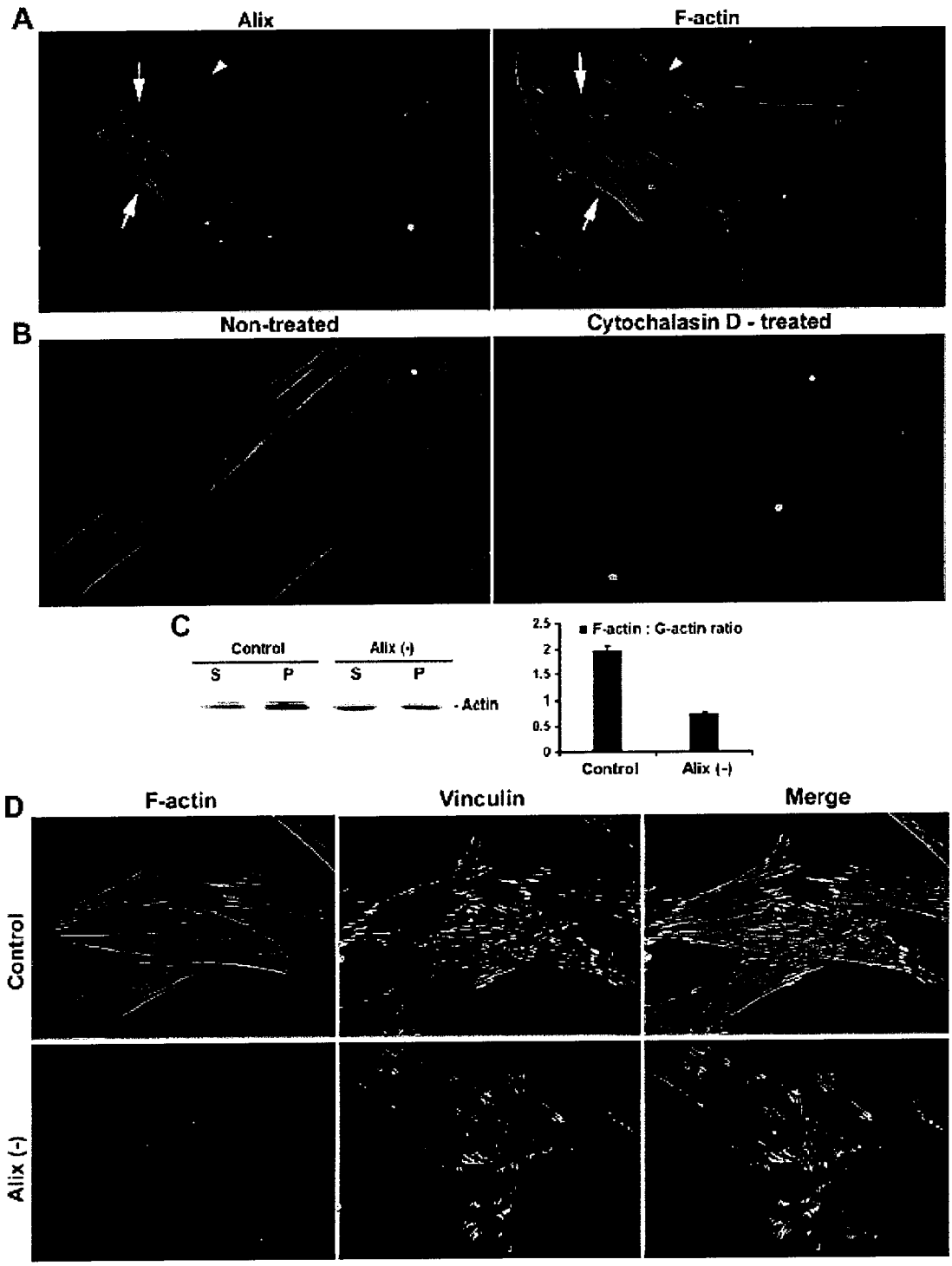
A
Alix
F-actin
B
Non-treated
Cytochalasin D - treated
C
Control
Alix (-)
S
P
S
P
- Actin
F-actin : G-actin ratio
2.5
2
1.5
1
0.5
0
Control
Alix (-)
D
F-actin
Vinculin
Merge
Control
Alix (-)

Figure 4

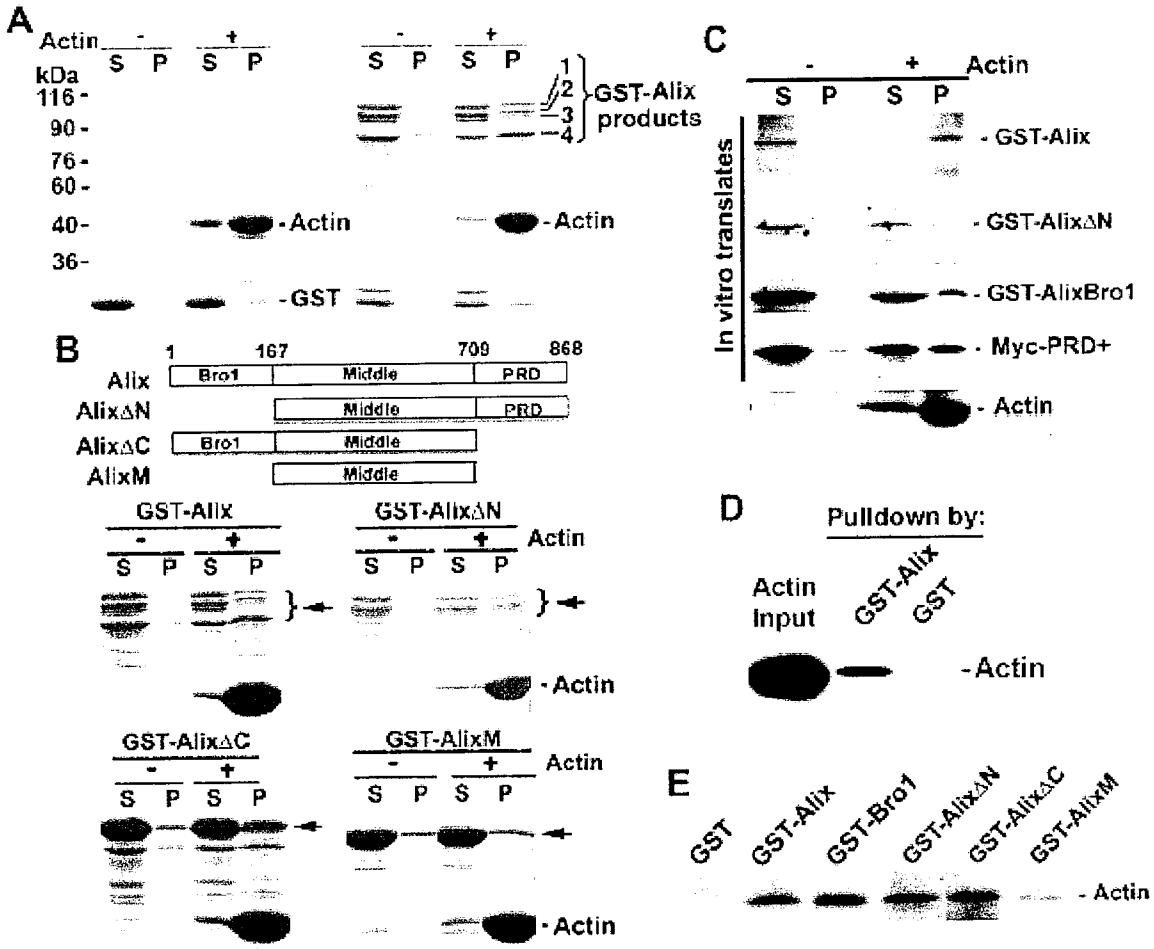
A
Actin
S P S P
kDa
116
90
76
60
40
36
1
2
3
4
GST-Alix products
Actin
GST
B
1 167 709 868
Alix
Bro1
Middle
PRD
AlixΔN
AlixΔC
AlixM
GST-Alix
GST-AlixΔN
GST-AlixΔC
GST-AlixM
C
Actin
In vitro translates
GST-Alix
GST-AlixΔN
GST-AlixBro1
Myc-PRD+
Actin
D
Pulldown by:
Actin Input
GST-Alix
GST
Actin
E
GST
GST-Alix
GST-Bro1
GST-AlixΔN
GST-AlixΔC
GST-AlixM
Actin

Figure 5

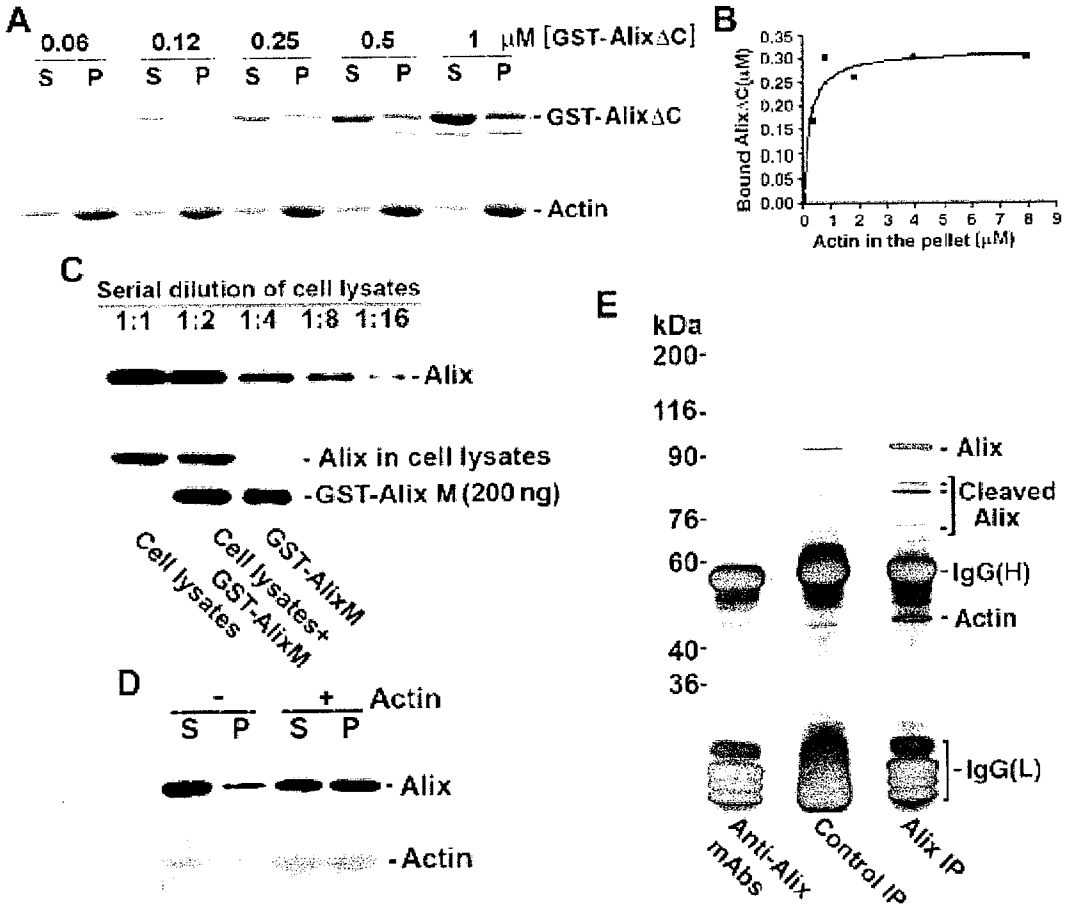
A
0.06
0.12
0.25
0.5
1 μM [GST-AlixΔC]
S P S P S P S P S P
- GST-AlixΔC
- Actin
B
Bound AlixΔC(μM)
Actin in the pellet (μM)
C
Serial dilution of cell lysates
1:1 1:2 1:4 1:8 1:16
- Alix
- Alix in cell lysates
- GST-Alix M (200 ng)
Cell lysates
Cell lysates+ GST-AlixM
GST-AlixM
D
- + Actin
S P S P
- Alix
- Actin
E
kDa
200-
116-
90-
76-
60-
40-
36-
- Alix
Cleaved Alix
- IgG(H)
- Actin
- IgG(L)
Anti-Alix mAbs
Control IP
Alix IP

Figure 6

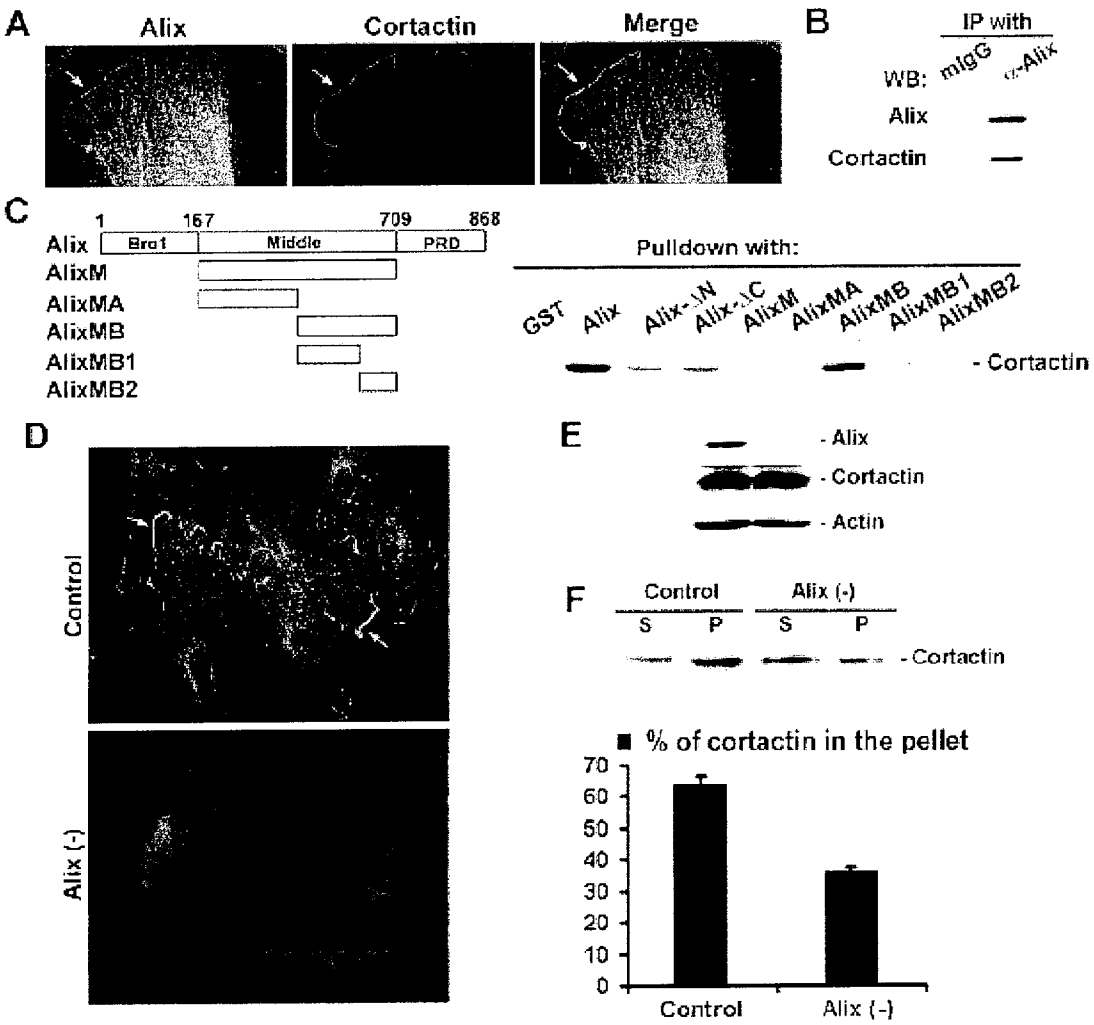
A
Alix
Cortactin
Merge
B
IP with
mIgG
α-Alix
WB:
Alix
Cortactin
C
1
167
709
868
Alix
Brα1
Middle
PRD
AlixM
AlixMA
AlixMB
AlixMB1
AlixMB2
Pulldown with:
GST
Alix
Alix-ΔN
Alix-ΔC
AlixM
AlixMA
AlixMB
AlixMB1
AlixMB2
- Cortactin
D
Control
Alix (-)
E
- Alix
- Cortactin
- Actin
F
Control
Alix (-)
S
P
S
P
- Cortactin
% of cortactin in the pellet
70
60
50
40
30
20
10
0
Control
Alix (-)

Figure 7

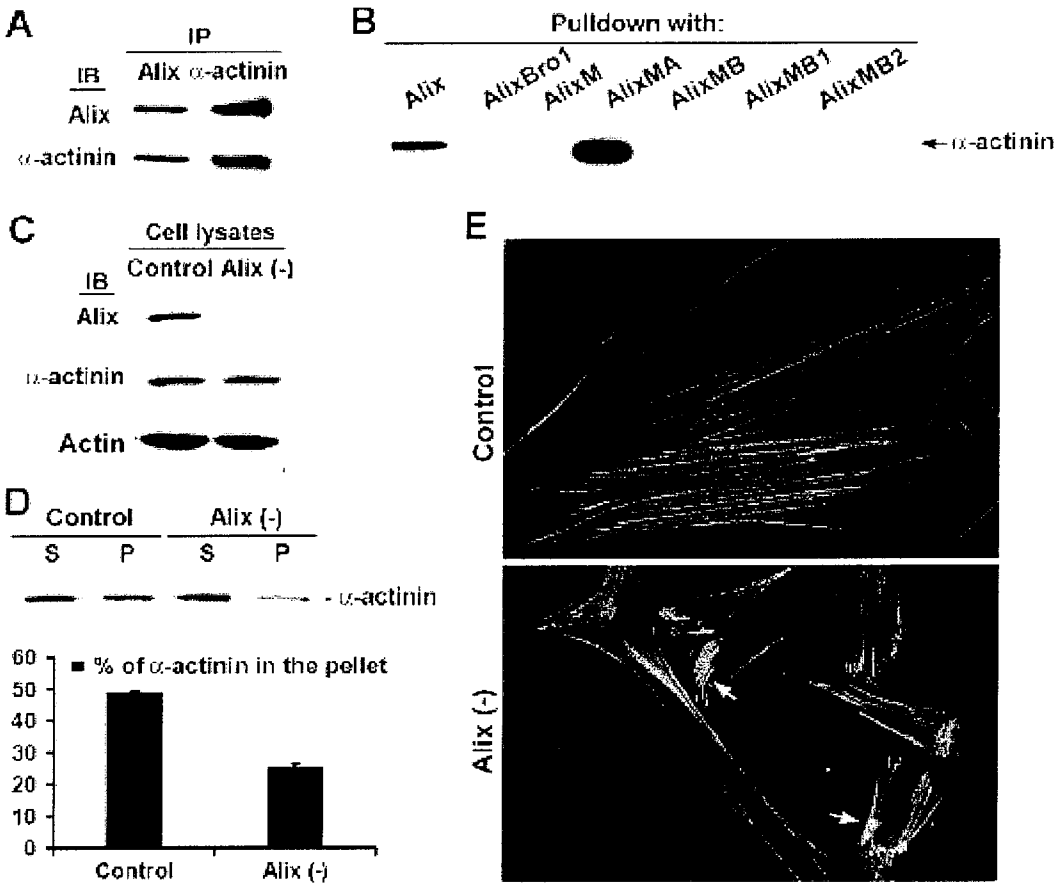
A
IP
IB
Alix α-actinin
Alix
α-actinin
B
Pulldown with:
Alix
AlixBro1
AlixM
AlixMA
AlixMB
AlixMB1
AlixMB2
←α-actinin
C
Cell lysates
IB
Control Alix (-)
Alix
α-actinin
Actin
D
Control
Alix (-)
S
P
S
P
α-actinin
60
50
40
30
20
10
0
% of α-actinin in the pellet
Control
Alix (-)
E
Control
Alix (-)

Figure 8

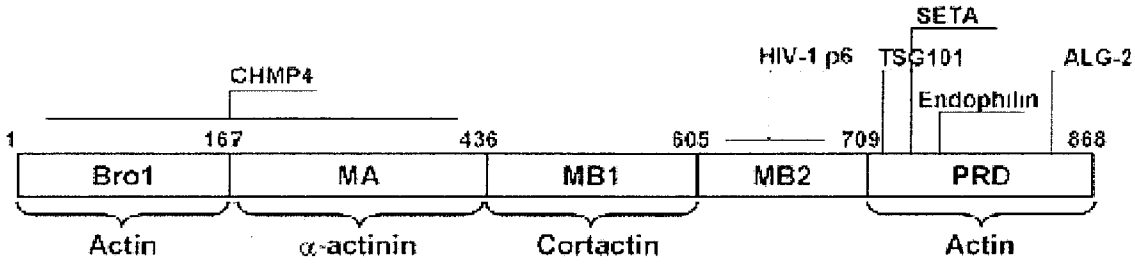

Figure 9

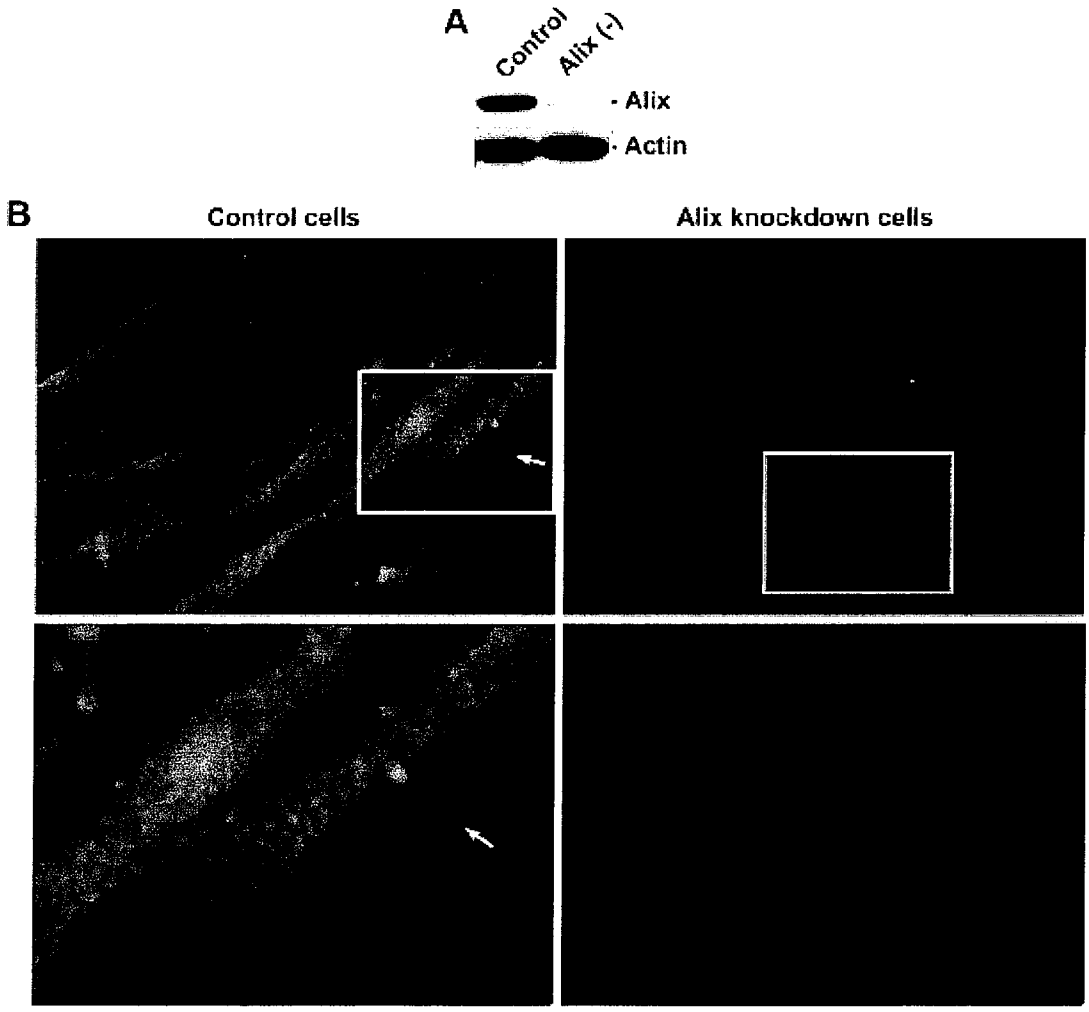

Figure 10

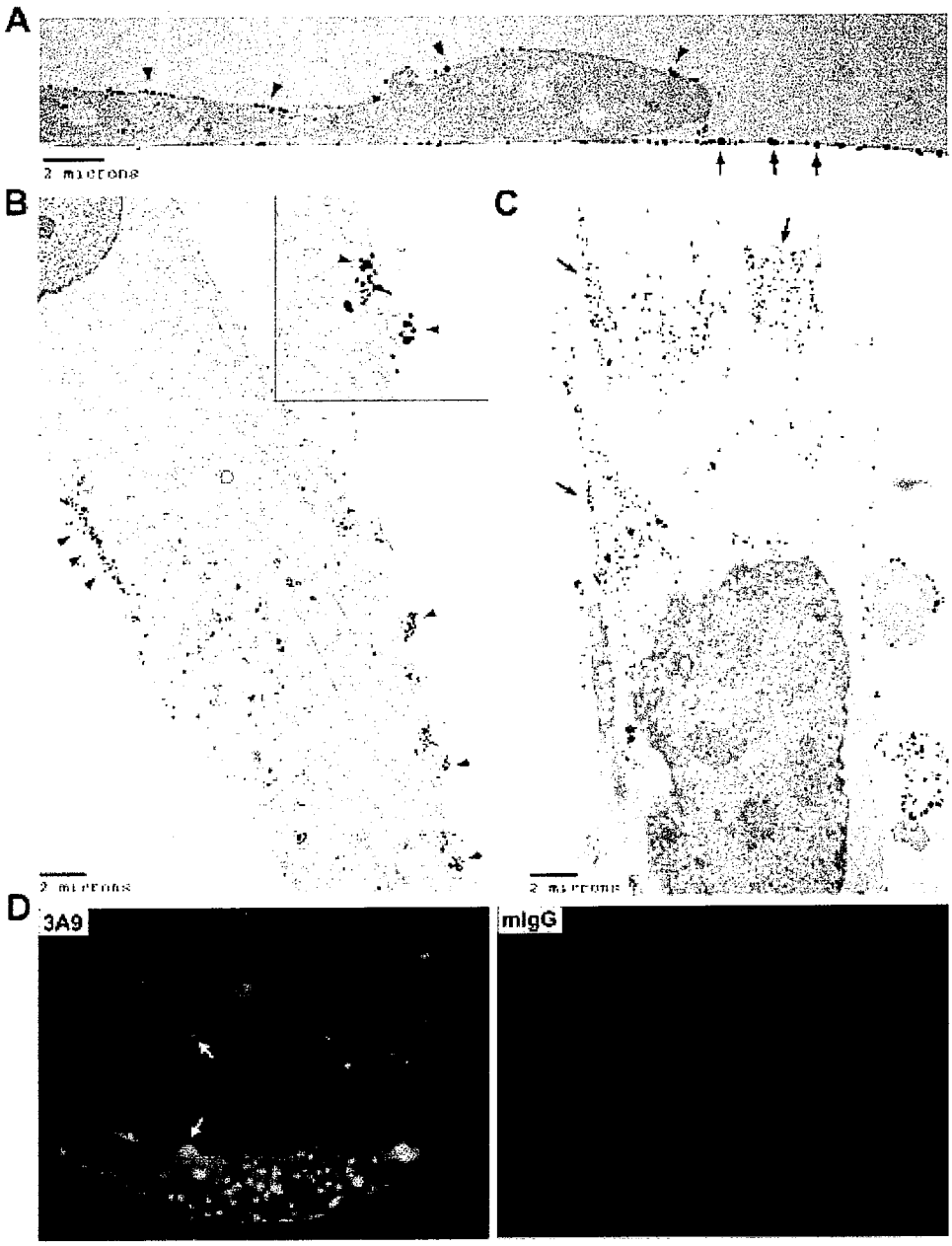

Figure 11

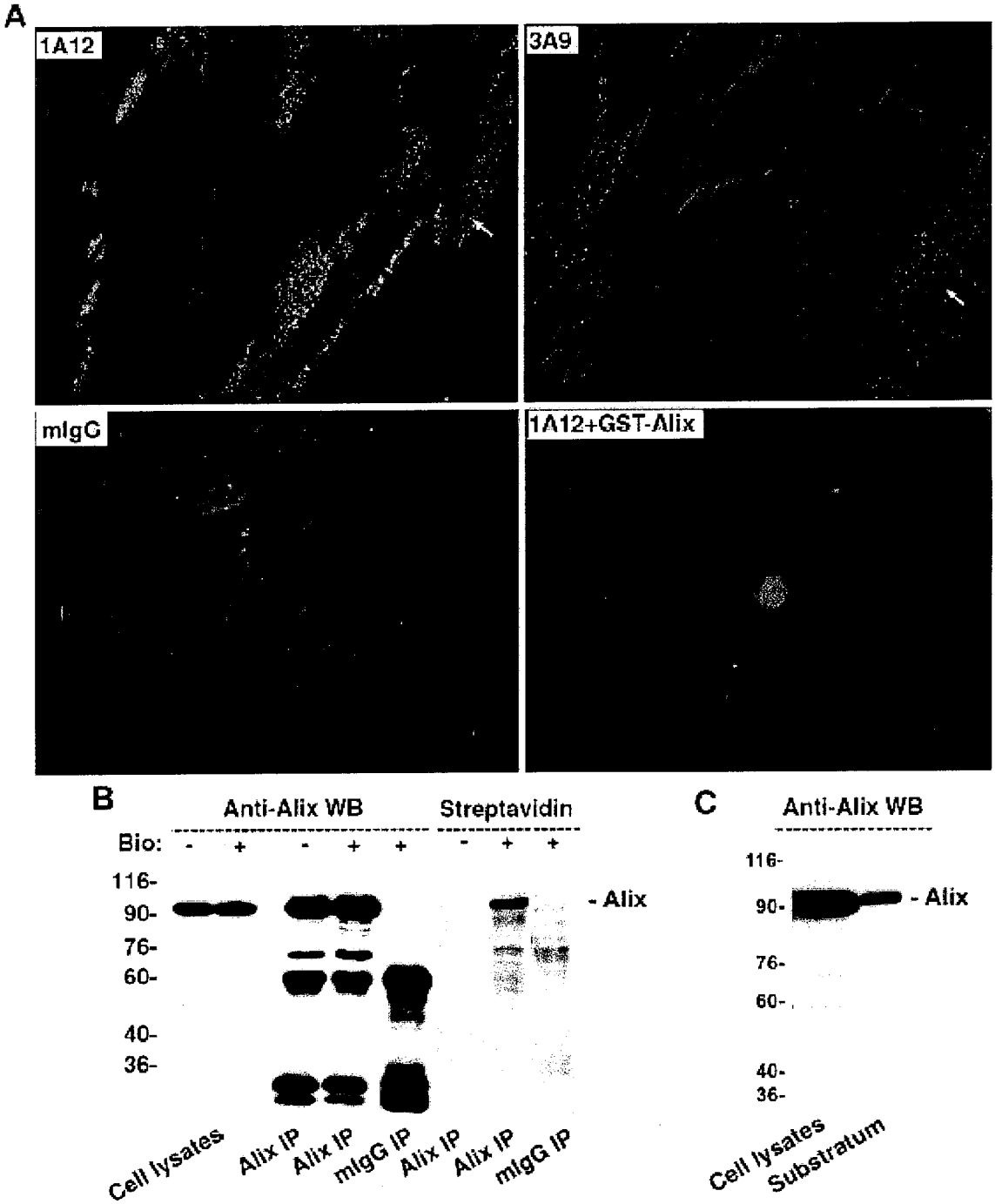
A
1A12
3A9
mIgG
1A12+GST-Alix
B
Anti-Alix WB
Streptavidin
Bio: - + - + + - + +
116-
90-
76-
60-
40-
36-
- Alix
Cell lysates
Alix IP
Alix IP
mIgG IP
Alix IP
Alix IP
mIgG IP
C
Anti-Alix WB
116-
90-
76-
60-
40-
36-
- Alix
Cell lysates
Substratum

Figure 12

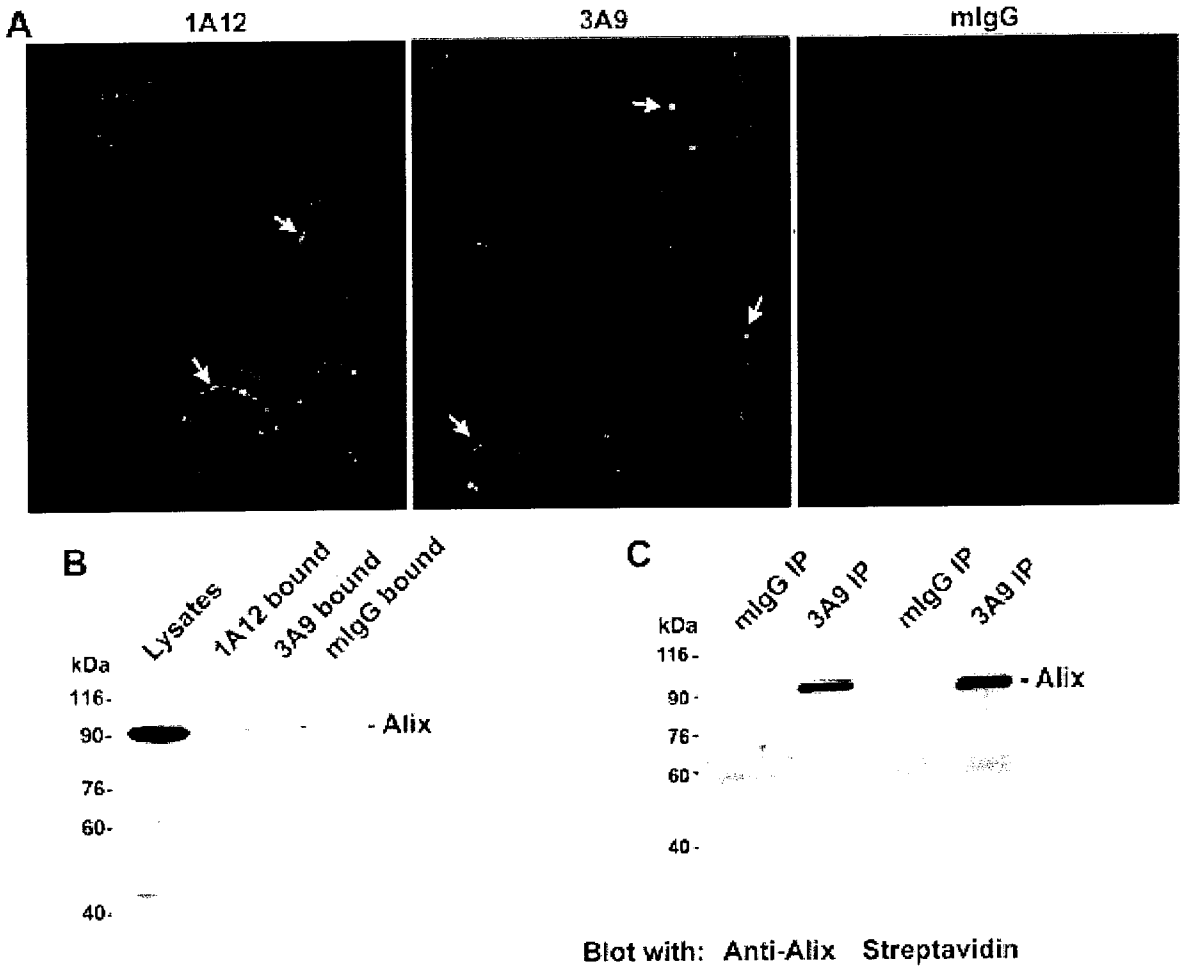
A
1A12
3A9
mIgG
B
Lysates
1A12 bound
3A9 bound
mIgG bound
kDa
116-
90-
76-
60-
40-
- Alix
C
mIgG IP
3A9 IP
mIgG IP
3A9 IP
kDa
116-
90-
76-
60-
40-
- Alix
Blot with: Anti-Alix Streptavidin

Figure 13

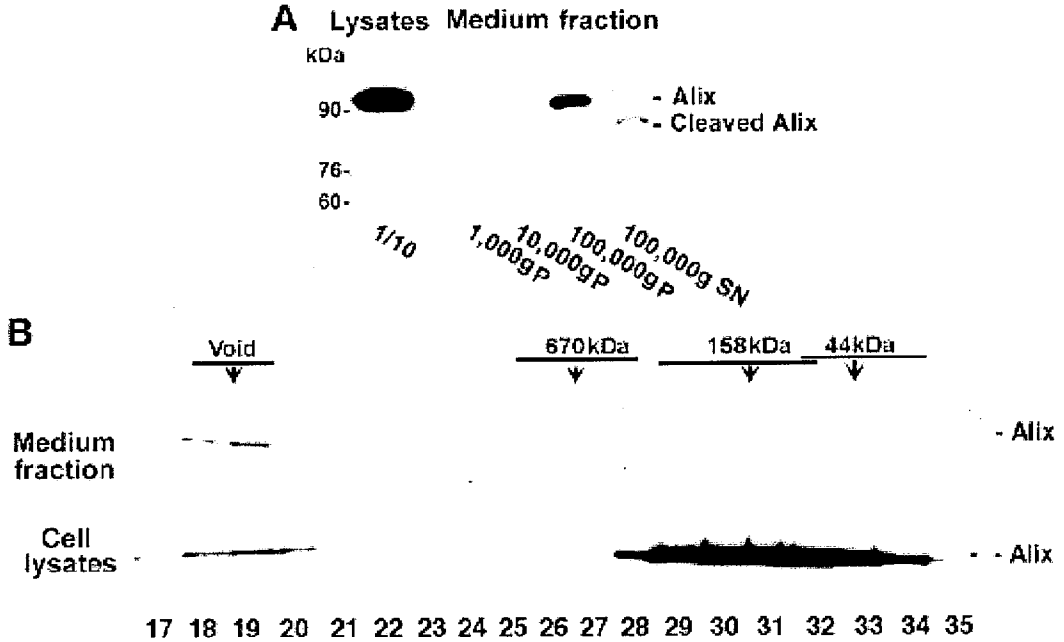

Figure 14

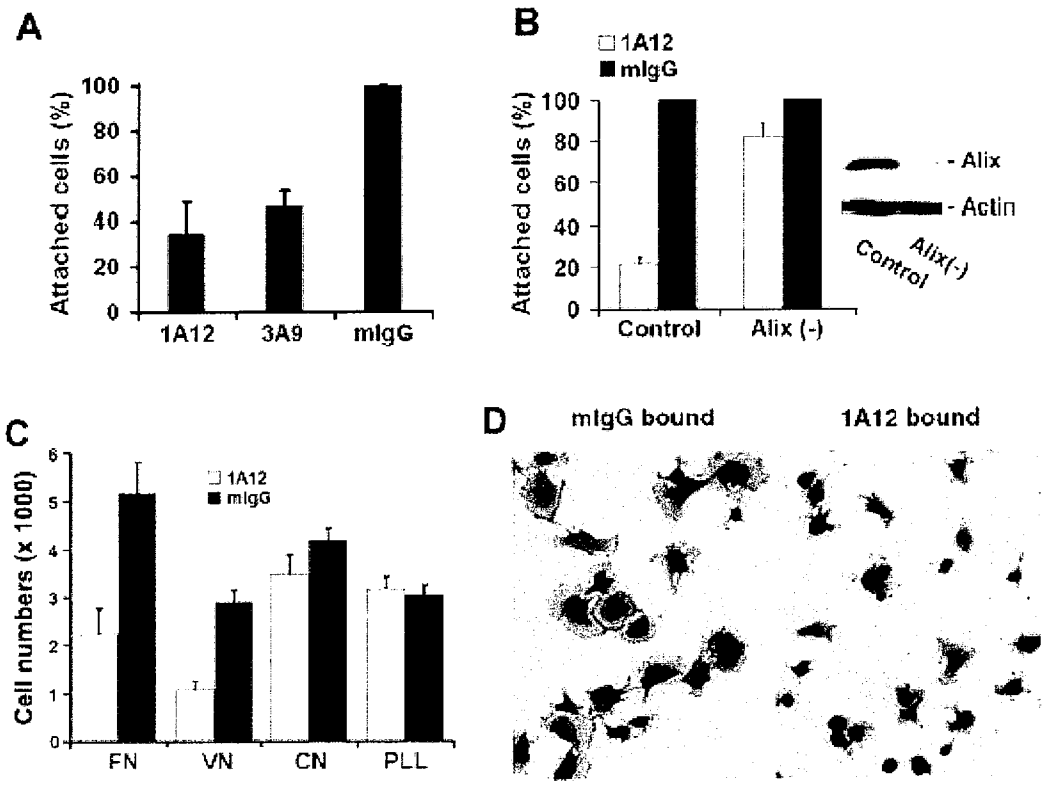

Figure 15

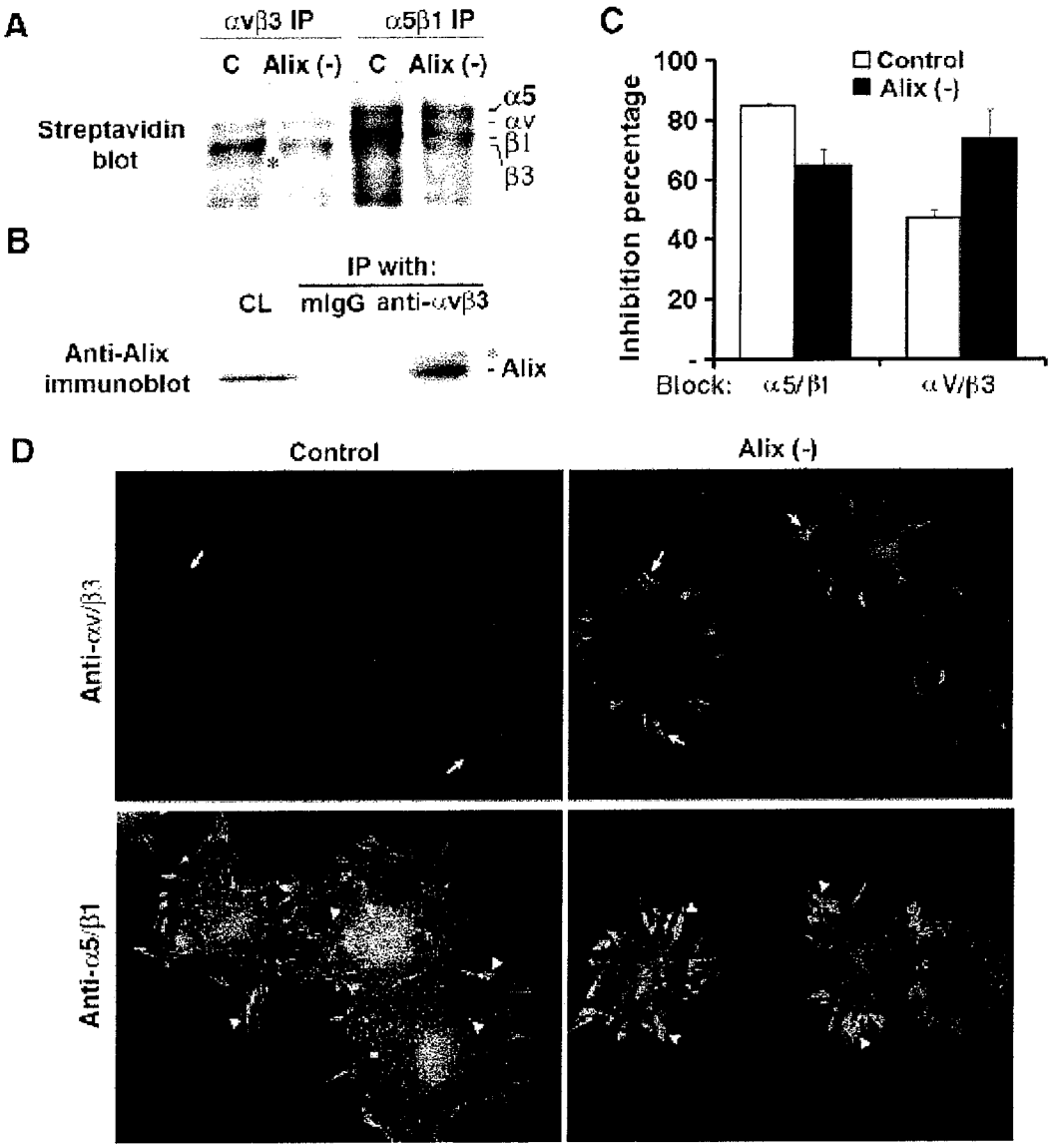
A
αvβ3 IP
α5β1 IP
C
Alix (-)
C
Alix (-)
Streptavidin blot
α5
αv
β1
β3
B
IP with:
CL
mIgG
anti-αvβ3
Anti-Alix immunoblot
Alix
C
Control
Alix (-)
Inhibition percentage
100
80
60
40
20
-
Block:
α5/β1
αV/β3
D
Control
Alix (-)
Anti-αv/β3
Anti-α5/β1

Figure 16

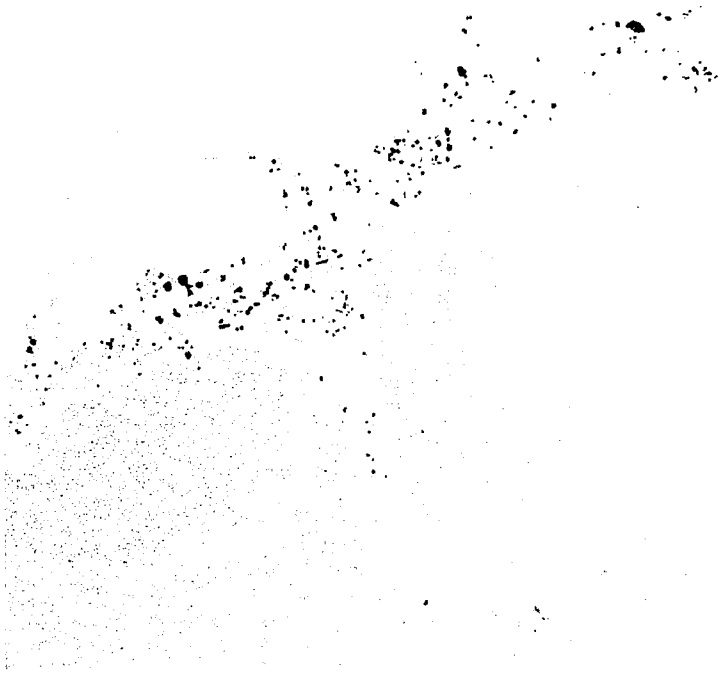

Figure 17

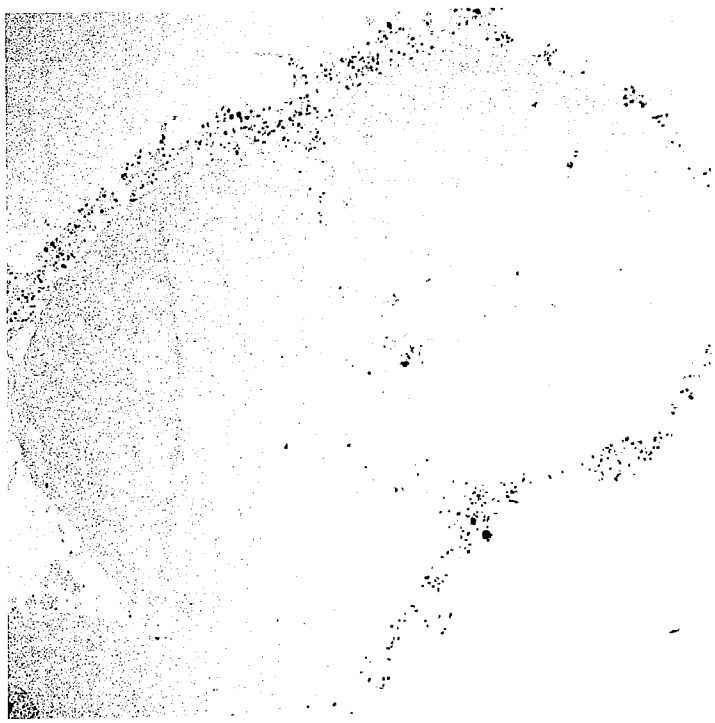

Figure 18